HSD2 neurons and the neural circuitry underlying sodium appetite

Brooke Jarvie

A dissertation
submitted in partial fulfillment of the
requirements for the degree of

Doctor of Philosophy

University of Washington
2018

Reading Committee:
Richard Palmiter, Chair
Sheri Mizumori
Daniel Storm

Program Authorized to Offer Degree:
Neuroscience

University of Washington

Abstract

HSD2 neurons and the neural circuitry underlying sodium appetite

Brooke Jarvie

Chair of the Supervisory Committee:
Richard Palmiter
Department of Biochemistry

Maintaining sodium homeostasis is critical for survival and is regulated by both dietary ingestion of salt and retention of sodium by the kidney. Beyond the hedonic aspects of sodium intake, animals will develop a voracious appetite for sodium when sodium-deprived and consume sodium at concentrations that are normally strongly aversive. The neural circuitry responsible for motivating this sodium appetite has not been clearly deciphered, although a population of aldosterone-sensitive neurons in the hindbrain have been identified as a likely part of the circuitry. These neurons express the enzyme 11β-hydroxysteroid dehydrogenase type II (HSD2), which is required for a cell to respond to aldosterone. Sodium appetite can be artificially induced with intracranial infusions of aldosterone, and the HSD2 neurons in the hindbrain are activated following a series of manipulations that induce sodium appetite. The purpose of this thesis is to show a causal role for HSD2 neurons in sodium appetite, and to and explore the role of their downstream projections.

Using a chemogenetic approach, we found that HSD2 neurons are both necessary and sufficient for sodium appetite, and do not regulate thirst. This appetite is specific for sodium, although activation of HSD2 neurons can decrease food intake. We confirmed the major downstream projections from the HSD2 neurons to unknown neurons in the bed nucleus of the stria terminalis (BNST), and to Foxp2 neurons in the parabrachial nucleus (PBN) and pre-locus coeruleus (pre-LC). However, activation of Foxp2 neurons was not sufficient to drive sodium intake but does appear to have a role in the regulation of thirst. More specific genetic markers are needed to further define the role of the PBN/pre-LC in sodium appetite and thirst. Collectively, these data start to functionally define how the body regulates sodium intake in order to maintain sodium homeostasis.

Table of Contents

Chapter 1

Introduction

The body is hard-wired to respond during a state of homeostatic crisis to coordinate physiological and behavioral responses that promote survival. How this is coordinated on a neurological level for any particular upset, such as deprivation of food, water, or sodium, has many important implications for disorders resulting from the malfunction of these systems. In the case of abnormal sodium intake, these disorders have fatal consequences. Thus, understanding the mechanisms that underlie intake of this essential nutrient is crucial to furthering the broad fields of biological science and medicine. Sodium homeostasis is maintained in two ways: through sodium retention in the kidney and dietary ingestion of salt. Under normal conditions, low concentrations of salt are appetitive. During a state of sodium deficiency, animals develop a voracious salt appetite that drives them to ingest salt at unusually large volumes or at concentrations that are normally strongly aversive[1]. The neural mechanisms that drive sodium-deficient animals to seek and consume typically aversive levels of salt remain poorly understood.

The overarching goal of this thesis is to contribute to our understanding of how the brain responds to dynamic peripheral signals during a state of need to maintain life. More specifically, this thesis focuses on defining the neural circuitry in the hindbrain that drives sodium intake during a state of sodium deficit. This introduction will describe critical aspects of the phenomenon of sodium appetite and explore the groundwork that led us to focus on the role of HSD2 neurons in sodium appetite. Chapter 2 is a published manuscript showing that HSD2 neurons are both necessary and sufficient for sodium appetite. Additional, unpublished follow-up experiments are described in Chapter 3, where I attempted to identify the function of neurons downstream of HSD2 neurons in the parabrachial nucleus (PBN) and pre-locus coeruleus (pre-

LC). The final chapter is a discussion and contextualization of my findings within the known neural circuitry underlying sodium appetite, including data from relevant papers published soon after Chapter 2's manuscript was published. Finally, there are two appendices included at the end of this document. These describe experiments completed with relation to the function of parabrachial neurons that is independent of salt appetite (**Appendix 1**), or likely independent of the HSD2 neuron-circuitry (**Appendix II**).

Sodium appetite

Sodium appetite is an important motivated behavior that helps maintain fluid homeostasis and occurs when there is a critical deficit in sodium that can threaten survival. Sodium levels in the body control extracellular fluid volume, and prolonged sodium deficiency can inhibit growth, reproduction, cognition and ultimately be lethal[2–4]. Under these depleted conditions, sodium is required to restore normal homeostasis, and water intake alone is insufficient. Animals show strong discriminatory intake for sodium as the result of a sodium deficient, and do not exhibit preferences for salts like potassium or the anions commonly paired with Na^+ (such as chloride or carbonate)[5–7]. It is unclear whether the neural circuitry underlying sodium appetite is distinct from need-free consumption, which is the daily intake of appetitive concentrations of salt that is thought to be a part of a hedonic circuitry where salt tastes pleasurable.

A defining characteristic of sodium appetite is that animals will dramatically increase their intake of previously aversive concentrations of sodium, and often will not only consume sodium in excess of need, but will also work to obtain it[8–10]. Additionally, following sodium depletion, rats find sodium more palatable and will shift their taste reactivity behavior from aversive to more appetitive[11]. This is interesting because the mechanisms underlying the detection of low and high concentrations of salt are different[12–15]. Salt attraction requires

expression of the amiloride-sensitive epithelial sodium channel (ENaC) on a subset of taste-receptor cells (TRCs) in mice, although loss of this channel has no impact on the avoidance of higher concentrations of salt[16]. Using calcium imaging in TRCs, Chandrashekar et al. [116] found that a subset of TRCs responded to both low and high concentrations of sodium, whereas a different subset responded non-selectively to high concentrations of various types of salt, and was not amiloride sensitive. However, sodium intake following sodium deprivation can be severely decreased following pre-treatment on the tongue with amiloride[17], suggesting that sodium appetite is primarily dependent on the processing of sodium by ENaC channels. Additionally, looking at a concentration-licking response curve, rats do not change their perception of the relative intensity of different sodium concentrations, but rather just ingest a greater volume of sodium solution at each concentration[18,19]. The overall perception of sodium taste does not change either, as a learned aversion to sodium interfered with sodium intake following sodium depletion[19]. Therefore, there appears to be a change in the motivational properties of salt, but not in the sensory identification and processing of sodium taste.

Exactly how the motivation to consume sodium and accompanying hedonic shift in sodium palatability occurs following sodium depletion is not clear, although there are a couple of regions in the brain that have been implicated. One of these regions is the nucleus accumbens (NAc), which broadly is important for motivation, aversion, and reward processing. Increased dopamine release in the NAc shell occurs selectively in response to the taste of sodium during sodium deprivation[20,21], and there are robust changes in the firing patterns of neurons in this region in response to salt during different need-states[22]. Similarly, there are clear increases in neural firing frequency following oral delivery of an aversive concentration of sodium in the ventral pallidum (VP) following sodium deprivation[23], which is a major downstream target of the

NAc and is thought to track the hedonic value of tastes[24]. Lesions or pharmacological inhibition of the VP can decrease saccharin intake and switch taste reactivity responses from positive to negative[25–27], although optogenetic inhibition of this regions prevents context-driven salt seeking but not consumption in sodium-deprived rats[28]. However, these data suggest that the VP may be an important site for the switch in the hedonic value of salt. Surprisingly, lesioning the major source of dopamine in the brain, the ventral tegmental area, does not have any effect on baseline sodium intake[29] or sodium appetite[30]. However, lesions of the lateral hypothalamus, or inhibition of dopamine receptors in this region, robustly inhibits sodium intake[30,31]. Following sodium depletion, rats will choose to consume salt rather than lever pressing for rewarding stimulation of the lateral hypothalamus[32]. There is a lot of work to be done to disentangle how each of these regions is involved in sodium appetite and encoding the value of salt.

Stimuli that induce sodium appetite: Aldosterone and Angiotensin II

A variety physiological peripheral signals occur in response to sodium depletion, including production of angiotensin II (Ang II) and the mineralocorticoid aldosterone. Both of these hormones are recruited when the kidney senses low blood pressure or decreased salt perfusion; they are part of a cascade (renin-angiotensin-aldosterone system) that works to return the body to a state of fluid homeostasis[3]. Renin is released from the kidney and stimulates release of a peptide precursor that is eventually cleaved into Ang II, which in turn promotes aldosterone release from the adrenal gland. Ang II causes vasoconstriction and increased blood pressure, and intracranial infusion is a potent stimulus for ingestion of water[33]. However, Ang II infusions can also stimulate sodium intake, and inhibition with antagonists or genetic knockout of one of the Ang II receptors (AT1a) can strongly attenuate or block sodium appetite[33–36]. Ang II is therefore

considered an important signaling mechanism for sodium appetite, although given that it has a role in the generation of thirst, its effect on sodium appetite can be complicated to interpret.

The actions of aldosterone are much more specific for sodium homeostasis. One of the primary roles of aldosterone is sodium retention at the level of the kidney; aldosterone promotes reabsorption of sodium and excretion of potassium, which in turn influences blood pressure and water retention. Loss of the adrenal glands leads to almost complete loss of sodium reabsorption, and animals develop a robust sodium appetite that is critical for survival[37,38]. Paradoxically, central infusions of aldosterone or other mineralocorticoids can elicits sodium intake, which unlike Ang II, appears to be independent of thirst[37,39–42]. Antagonists for the mineralocorticoid receptor (MR) can attenuate need-based salt intake[35,40]. Therefore, aldosterone controls both retention of sodium and dietary ingestion of salt, and this historically made aldosterone-sensitive neurons an ideal candidate for identifying neurons involved in sodium appetite[43].

Aldosterone binds to MRs, which also bind glucocorticoids with equal or greater affinity[44,45]. Given that glucocorticoids circulate at levels 100-1000 times greater than aldosterone, most cells that express the MR are insensitive to changes in aldosterone, because most MRs are already occupied by glucocorticoids. Therefore, for a cell to be aldosterone-sensitive, it must also express the enzyme 11-β-hydroxysteroid dehydrogenase type II (HSD2), which metabolizes glucocorticoids to an inert form that no longer bind to MRs[46–48]. Conditional deletion of HSD2 in the brain in mice results in increased sodium appetite[49], as do mutations in the gene encoding for HSD2 in humans[50].

HSD2 neurons

HSD2-expressing neurons are predominately located in the nucleus of the solitary tract (NTS)[43,51]. In rats, HSD2 expression has also been reported in the ventral medial hypothalamus (VMH), scattered throughout the medial vestibular nucleus, and ependymal cells forming the subcommisural organ, although co-expression of the MR and HSD2 has only been reported in the NTS[43,52,53]. In mice, HSD2 appears to be exclusively expressed in the NTS, where it also co-localizes with MRs[51,54]. These results support behavioral data showing that chronic aldosterone infusions into the 4th ventricle of the hindbrain, but not the forebrain, increases sodium intake[40]. These HSD2 neurons in the NTS have been well characterized with regard to sodium appetite, as they only express Fos following stimuli related to sodium appetite, including dietary sodium deprivation, chronic infusion of mineralocorticoids, and adrenalectomy[42,55,56].

HSD2 neurons are well placed to integrate multiple incoming signals to both drive and inhibit sodium intake. These neurons are located in region of the NTS that appears to have fenestrated capillaries and greater permeability of the blood-brain barrier, which allow circulating hormones such as aldosterone and Ang II to access the NTS[51,57,58]. A recent electrophysiology study demonstrated that aldosterone application to a brain slice does not induce acute activation of HSD2 neurons, but mice that have been chronically treated with aldosterone prior to tissue collection did show an elevated firing frequency in HSD2 neurons compared to controls[59]. Taking a closer look at behavior data, many of the studies demonstrating the effects of mineralocorticoids on sodium appetite have used chronic, supraphysiological doses[1]. Studies using acute or physiological doses produce mild or negligible salt intake, suggesting that aldosterone may normally act to enhances sodium intake over time, rather than causing rapid response in intake[5,60,61]. HSD2 neurons also express Ang II receptors and increase their firing rate in response to bath application of receptor agonists to slices[51,59]. Therefore,

referring to these neurons as just aldosterone-sensitive may be misleading, as they appear to respond to multiple inputs that occur during a sodium-depleted state, including Ang II.

Histological studies have also suggested that HSD2 neurons receive various synaptic inputs that would allow them to respond to other peripheral signals. Using a transganglionic anterograde tracer, it appears that HSD2 neurons receive input from the vagus nerve, specifically relaying information from the stomach[62,63]. Interestingly, rats with intragastric fistulas drink greater amounts of sodium following sodium depletion than controls[64], suggesting that there is a post-ingestive negative feedback signal that normally regulates sodium intake and either overrides or turns off the motivational state that occurs during sodium deprivation. Saline intake also rapidly decreases Fos in HSD2 neurons following treatment with mineralocorticoids or dietary sodium depletion[42,56]. Optogenetic activation of inputs to the NTS from the nodose ganglion of the vagus activated non-HSD2 neurons, with a delayed change in firing of HSD2 neurons[59]. This suggests that HSD2 neurons do not receive direct vagal innervation but may receive indirect input from other neuronal populations within the NTS. There is histological evidence to suggest that HSD2 neurons do receive input from neighboring cells, as well as direct or indirect input from putatively sodium-sensing neurons in the nearby area postrema (AP)[65]. The AP has been shown to have a strong inhibitory effect on sodium appetite through lesion studies[66,67], which could in part be mediated by inhibition of HSD2 neurons. Overall, HSD2 neurons appear to receive a myriad of inputs that can both drive or inhibit sodium intake, depending on the state of need.

Sodium appetite in humans

There are many examples of sodium appetite in humans, although it has been argued that the appetite exhibited by humans is not as straightforward as seen in other mammals. While

humans find salt intake appetitive and ingest it in excess of need, following sodium depletion humans do not try to ingest sodium in its pure form, or with the same level of discrimination for salty foods as reported in other animals[68,69]. Instead, humans experience an increase in the palatability of sodium, and demonstrate a preference for salted food. Increased salt preference and consumption has been demonstrated in patients with congenital adrenal hyperplasia 21-hydroxylase deficiency (CAH)[70], and linked to perinatal sodium loss that can occur with maternal vomiting or infant vomiting/diarrhea[70,71]. In adults, changes in fluid balance following exercise[72,73] and dialysis have been shown to increase sodium preference[74]. Therefore, alteration of sodium balance in humans can influence dietary choices with regard to salt.

Sodium overconsumption is a more prevalent concern than sodium deprivation in the average human population due to the high occurrence of salt in global diets. Excess sodium ingestion can have detrimental effects and has been strongly linked to cardiovascular diseases and related deaths[75–77]. Restriction of sodium intake can also be beneficial for controlling symptoms in patients with heart failure, kidney failure, and salt-sensitive hypertension[78–80], where some patients may also exhibit an increase in sodium cravings. However, patients can be notoriously poor at decreasing their salt intake[81–83]. A more complete understanding of the drive to consume sodium and the neural circuitry underlying it may provide insight in how to help patients decrease cravings for salt.

Chapter 2

HSD2 Neurons in the hindbrain drive sodium appetite

*This chapter was published with minor reformatting as an article with the same title in Nature Neuroscience. The full citation is as follows:

Jarvie, B.C. & Palmiter, R.D. HSD2 neurons in the hindbrain drive sodium appetite. *Nat Neurosci*. **20,** 167-169 (2017).

Abstract

Sodium-depleted animals develop an appetite for aversive concentrations of sodium. Here we show that chemogenetic activation of aldosterone-sensitive neurons which express 11β-hydroxysteroid dehydrogenase type 2 (HSD2) in the nucleus of the solitary tract is sufficient to drive consumption of sodium-containing solutions in mice, independently of thirst or hunger. These HSD2-positive neurons are necessary for full expression of sodium appetite, and have distinct downstream targets that are activated during sodium depletion.

HSD2 Neurons in the hindbrain drive sodium appetite

Brooke C. Jarvie[1], Richard D. Palmiter[1,2]

[1]Department of Biochemistry, University of Washington, Seattle, Washington, USA
[2]Howard Hughes Medical Institute, University of Washington, Seattle, Washington, USA
Correspondence should be addressed to B.C.J (bcjarvie@uw.edu) or R.D.P. (palmiter@uw.edu)

Hunger and thirst are profound motivated states produced by physiological need, and great strides have been taken to identify the neural circuitry underlying both eating and drinking[84–86]. However, more specific physiological needs can also impact consumption behavior. For example, sodium intake is critical for survival and during a state of sodium depletion, animals will consume sodium at concentrations that are normally strongly aversive[1]. This phenomenon is termed a sodium appetite and can be artificially induced by injection of aldosterone into the hindbrain[40]. This is likely due to a population of neurons in the nucleus of the solitary tract (NTS) which expresses both the mineralocorticoid receptor (MR) and the enzyme 11β- hydroxysteroid dehydrogenase type 2 (HSD2), making these neurons uniquely responsive to aldosterone (**Supplementary Fig. 1**)[43,48].

To determine the role of HSD2 neurons in sodium appetite, we generated mice with Cre recombinase targeted to the gene *Hsd11b2* that encodes HSD2 (*Hsd11b2*^{Cre}; **Supplementary Fig. 1**). We targeted these neurons in the NTS by stereotaxically injecting a Cre-dependent adeno-associated virus that drives expression of the excitatory G-protein-coupled receptor hM3Dq fused to mCherry[87] (AAV1-DIO-hM3Dq:mCherry; **Fig. 1a**). We activated HSD2 neurons with peripheral injections of the physiologically inert ligand for hM3Dq, clozapine-N-oxide (CNO, **Supplementary Fig. 2**). Male hM3Dq-expressing mice drank significantly more of

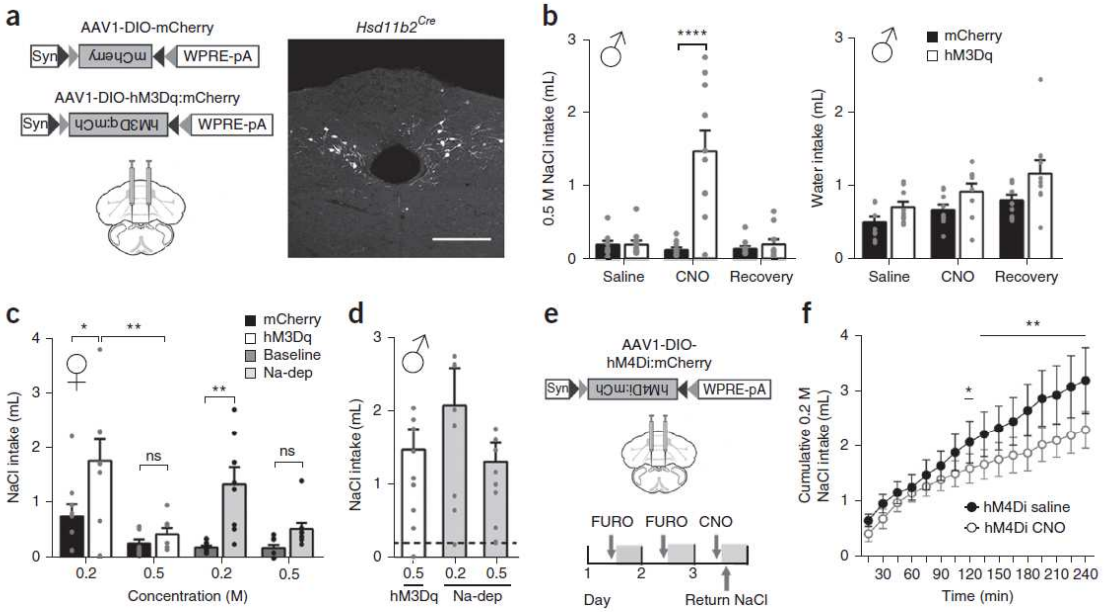

Figure 1 HSD2 neurons generate a sodium appetite independently of thirst. (**a**) Stereotaxic delivery of Cre-dependent hM3Dq:mCherry (hM3Dq) or mCherry into the NTS of *Hsd11b2*^{Cre} mice. Scale bar, 200 µm. (**b**–**f**) Two-bottle choice tests for intake of (**b**) NaCl and water during the first 4 h of the dark cycle in response to intraperitoneal injection of saline or CNO and during the first 4 h of the night following CNO treatment (recovery). Two-way ANOVA, *post hoc* Sidak's multiple comparisons test. (**c**) Sodium solution intake in response to CNO in female mice expressing mCherry or hM3Dq: mCherry in HSD2 neurons, or in wild-type mice before (baseline) and after sodium depletion (Na-dep). Two-way ANOVA, *post hoc* Sidak's multiple comparisons test. (**d**) No difference in hM3Dq-stimulated intake in male mice compared to wild-type, sodium-depleted mice. One-way ANOVA, *post hoc* Tukey test. Dotted line, average baseline intake of all three groups (0.211 ± 0.042 g). (**e**–**f**) Following sodium depletion, a combined group of male and female mice expressing hM4Di:mCherry in HSD2 neurons decreased their NaCl intake in response to CNO (repeated-measures ANOVA, *post hoc* Sidak's multiple comparisons test). FURO, furosemide injections. Error bars are s.e.m. $*P < 0.05$, $**P < 0.01$, $****P < 0.0001$. Exact *P*-values of all statistical tests are contained in **Supplementary Table 1**.

an aversive concentration of sodium chloride, but not water, compared to AAV1-DIO-mCherry controls in response to CNO (**Fig. 1b**). In rats, prior induction of a sodium appetite can increase subsequent *ad libitum* sodium intake[88], but we observed no lasting effect on sodium or water intake 24 h following CNO administration ("Recovery", **Fig. 1b**). The lack of change in water intake suggests that HSD2 neurons do not directly influence fluid homeostasis by affecting release of hormones like vasopressin or angiotensin II[89]. Female *Hsd11b2*^{Cre} mice also displayed a salt appetite in response to HSD2 neuron activation, although they responded better to a lower concentration of sodium chloride (0.2 M), which mimics the appetite induced in sodium-depleted female mice[90] (**Fig. 1c**). By contrast, sodium chloride concentration had no effect on the volume consumed by male mice (**Fig. 1d**). These data indicate that activation of HSD2 neurons is sufficient to induce a sodium appetite that is comparable to that seen following sodium depletion, without influencing thirst.

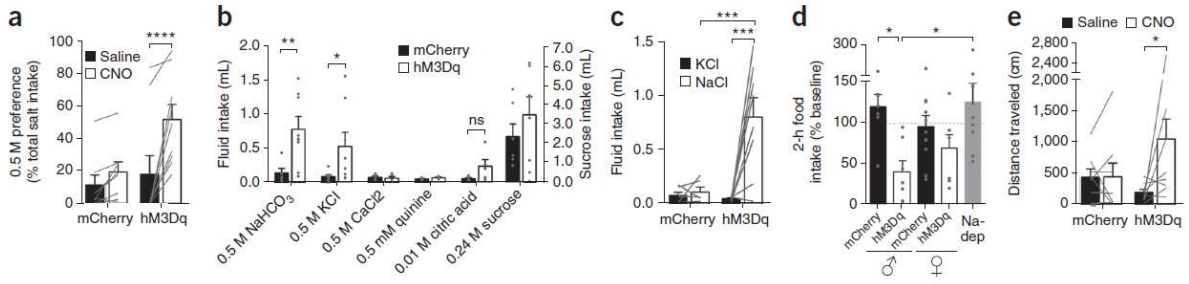

Figure 2 The appetite induced by HSD2 neurons is specific for sodium. (**a**) Preference for 0.5 M NaCl when given a choice between 0.5 M and 75 mM NaCl in *Hsd11b2*^{Cre} mice expressing either mCherry or hM3Dq:mCherry (hM3Dq) in the NTS (repeated-measures ANOVA, *post hoc* Sidak's multiple comparisons test). (**b**) Two-bottle taste test of various tastants in response to CNO (all tastants but sucrose: two-way ANOVA, *post hoc* Sidak's multiple comparisons test; sucrose: two-tailed, unpaired *t*-test). (**c**) Three-bottle taste test comparing 0.5 M NaCl and 0.5 M KCl intake following CNO administration, with water also available (repeated-measures ANOVA, *post hoc* Sidak's multiple comparisons test). (**d**) Male hM3Dq mice ate significantly less food in response to CNO than mCherry controls or wild-type mice that were sodium depleted (Na-dep). Female mice showed no significant change in their food intake (one-way ANOVA, *post hoc* Tukey test). (**e**) Increase in locomotion in response to CNO (repeated-measures ANOVA, *post hoc* Sidak's multiple comparisons test). Error bars are s.e.m. $*P < 0.05$, $**P < 0.01$, $***P < 0.001$. Exact *P*-values of all statistical tests are contained in **Supplementary Table 1**.

To test whether HSD2 neurons are necessary for sodium appetite, we acutely inhibited them using the CNO-responsive, inhibitory receptor hM4Di[87]. Following sodium depletion, CNO administration resulted in a small but significant decrease in intake of 0.2 M NaCl in a group of male and female hM4Di-expressing mice compared to those same mice injected with saline (**Fig. 1e-f**). CNO had no effect in mCherry-expressing mice (**Supplementary Fig. 3**). We verified hM4Di inhibition of HSD2 neurons by showing a decrease in sodium-depletion induced Fos expression in the NTS following CNO administration (**Supplementary Fig. 3**). We also irreversibly blocked vesicular neurotransmission in HSD2 neurons using a virus expressing the tetanus toxin light chain[91] (AAV1-DIO-GFP:TetTox). However, ~ 8 d after injection, mice lost ≥20% body weight and needed to be euthanized (**Supplementary Fig. 4**), suggesting that HSD2 neurons may have other important functions, e.g., cardiovascular regulation[49].

To investigate the specificity of the salt appetite induced by activating HSD2 neurons, we performed taste tests with a series of solutions. When given a choice, hM3Dq-expressing mice increased their consumption of an aversive, high concentration of sodium chloride (0.5 M) rather than a less concentrated, more appetitive solution (75 mM) following CNO injection (**Fig. 2a**). The hM3Dq-expressing mice also drank more 0.5 M sodium bicarbonate and 0.5 M potassium

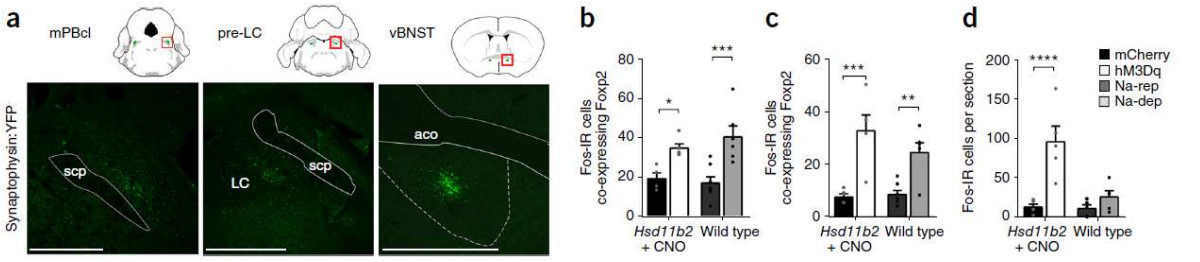

Figure 3 Efferent projections from HSD2 neurons. (**a**) AAV1-DIO-Synaptophysin:YFP injected into the NTS of *Hsd11b2*^{Cre} mice fluorescently labeled terminals in the medial subdivision of the central lateral parabrachial nucleus (mPBcl), pre-locus coeruleus (pre-LC) and ventral bed nucleus of the stria terminalis (BNSTv). Scale bar, 200 µm. (**b–d**) Both sodium depletion (Na-dep, wild-type mice) and chemogenetic stimulation of HSD2 neurons (CNO, *Hsd11b2*^{Cre} (hM3Dq) mice) increased Fos immunoreactivity (IR) in Foxp2-expressing cells in (**b**) mPBcl and (**c**) pre-LC compared to either mCherry or sodium-replete (Na-rep) controls. (**d**) Quantification of Fos IR in BNSTv, directly under fluorescently labeled fibers. All statistics were done using multiple unpaired, two-tailed *t*-tests with a *post hoc* Holm-Sidak test. Aco, anterior commissure; scp, superior cerebellar peduncle; LC, locus coeruleus. Error bars are s.e.m. $*P < 0.05$, $**P < 0.01$, $***P < 0.001$, $****P < 0.0001$. Exact *P*-values of all statistical tests are contained in **Supplementary Table 1**.

chloride than control mice following CNO stimulation, but not an alternative essential dietary cation, 0.5 M $CaCl_2$ **(Fig. 2b).** Mice may perceive KCl as a partial substitute for NaCl, as wild-type mice also increased KCl intake following our sodium depletion protocol, unlike rats[92]. (**Supplementary Fig. 5**). However, when given a choice, mice chose NaCl over KCl following HSD2 neuron activation (**Fig. 2c**). Activation of HSD2 neurons did not affect intake of any other solutions tested, including tastants that were sour (10 mM citric acid), bitter (10 mM quinine-HCl) or sweet (0.24 M sucrose) (**Fig. 2b**). In addition, mice did not alter their water intake during any of the two-bottle assays (**Supplementary Fig. 6**). Chemogenetic stimulation of HSD2 neurons attenuated consumption of low-sodium chow in males but not females, relative to control mice, but sodium depletion did not reduce food intake in wild-type male mice (**Fig. 2d**). Perhaps only during extreme sodium depletion would anorexia be observed. Additionally, only subtle changes in locomotion occurred following HSD2 neuron activation (**Fig. 2e**), unlike the robust foraging-like behavior seen in starving mice or after stimulation of hunger-related neurons in the hypothalamus[93].These data demonstrate that activation of HSD2 neurons creates a motivated state that drives sodium consumption but does not stimulate hunger.

Injection of AAV1-DIO-synaptophysin:YFP into HSD2 neurons in the NTS revealed three distinct terminal fields, including the ventral bed nucleus of the stria terminalis (BNSTv),

the medial subdivision of the central lateral parabrachial nucleus (mPBcl) and the pre-locus coeruleus (pre-LC, **Fig. 3a, Supplementary Fig. 9**), similar to the projections observed in rats[94]. Stimulation of HSD2 neurons led to Fos expression in all three projection sites, although following sodium depletion Fos expression was only observed in the mPBcl and pre-LC (**Fig 3b-d, Supplementary Fig. 7-9**). Previous studies have shown that sodium-depletion induced Fos expression in the parabrachial nucleus (PBN) and pre-LC is specific to Foxp2-expressing neurons[95], which we also see following either HSD2 neuron stimulation or sodium depletion (**Fig. 3b-c, Supplementary Fig. 8-9**). Activation of a different set of parabrachial neurons is presumably responsible for the strong inhibitory effect on sodium appetite that is normally attributed to the PBN[96].

These data demonstrate that HSD2 neurons in the NTS are sufficient to drive a motivated behavior that is distinct from thirst and hunger, but still fulfills an imperative physiological need. However, inhibition of HSD2 neurons only partially suppresses sodium intake, indicating that while these neurons are important for the full expression of sodium appetite, they are not absolutely necessary for sodium appetite to develop. This is likely due to redundant circuitry as is observed in feeding circuits[97], perhaps via the subfornical organ[85,98]. Development of a sodium appetite is particularly interesting because it overrides a naturally aversive response of 0.5 M NaCl to generate an appetitive response, but whether the circuitry that drives salt appetite also applies to hedonic consumption of salt is not clear. Overall, our data indicate that HSD2 neurons in the NTS increase salt intake and likely contribute to the development of sodium appetite, and hyper-activation of these neurons could contribute to dietary overconsumption of sodium in humans.

Accession Codes: None.

Acknowledgments: We thank K. Kafer and M. Chiang for help generating and maintaining the *Hsd11b2*^{Cre} mouse line. We thank H. King for assistance with behavior and histology. We thank the Palmiter laboratory and J. Schulkin for discussion and critiques. This work was supported by the National Science Foundation Graduate Research Fellowship under (DGE-1256082, B.C.J). Any opinion, findings, and conclusions or recommendations expressed in this material are those of the authors and do not necessarily reflect the views of the National Science Foundation.

Author Contributions: B.C.J. designed experiments under the guidance of R.D.P., B.C.J. performed and analyzed experiments. B.C.J. and R.D.P. wrote the manuscript.

Competing Financial Interests: Authors declare no competing financial interests.

References

1. Geerling, J. C. & Loewy, A. D. Central regulation of sodium appetite. *Exp. Physiol.* **93,** 177–209 (2008).

40. Formenti, S. *et al.* Hindbrain mineralocorticoid mechanisms on sodium appetite. *Am. J. Physiol. Regul. Integr. Comp. Physiol.* **304,** R252-9 (2013).

43. Geerling, J. C., Kawata, M. & Loewy, A. D. Aldosterone-sensitive neurons in the rat central nervous system. *J. Comp. Neurol.* **494,** 515–27 (2006).

48. Chapman, K., Holmes, M. & Seckl, J. 11β-hydroxysteroid dehydrogenases: intracellular gate-keepers of tissue glucocorticoid action. *Physiol. Rev.* **93,** 1139–206 (2013).

49. Evans, L. C. *et al.* Conditional Deletion of Hsd11b2 in the Brain Causes Salt Appetite and Hypertension. *Circulation* **133,** 1360–70 (2016).

84. Luquet, S., Perez, F. a, Hnasko, T. S. & Palmiter, R. D. NPY/AgRP neurons are essential for feeding in adult mice but can be ablated in neonates. *Science* **310,** 683–5 (2005).

85. Oka, Y., Ye, M. & Zuker, C. S. Thirst driving and suppressing signals encoded by distinct neural populations in the brain. *Nature* **520,** 349–52 (2015).

86. Aponte, Y., Atasoy, D. & Sternson, S. M. AGRP neurons are sufficient to orchestrate feeding behavior rapidly and without training. *Nat. Neurosci.* **14,** 351–5 (2011).

87. Rogan, S. C. & Roth, B. L. Remote control of neuronal signaling. *Pharmacol. Rev.* **63,** 291–315 (2011).

88. Sakai, R. R., Frankmann, S. P., Fine, W. B. & Epstein, A. N. Prior episodes of sodium depletion increase the need-free sodium intake of the rat. *Behav. Neurosci.* **103,** 186–92 (1989).

89. Antunes-Rodrigues, J., De Castro, M., Elias, L. L. K., Valença, M. M. & McCann, S. M. Neuroendocrine Control of Body Fluid Metabolism. *Physiol. Rev.* **84,** (2004).

90. Dadam, F. M. *et al.* Effect of sex chromosome complement on sodium appetite and Fos-immunoreactivity induced by sodium depletion. *Am. J. Physiol. Regul. Integr. Comp. Physiol.* **306,** R175-84 (2014).

91. Kim, J. C. *et al.* Linking Genetically Defined Neurons to Behavior through a Broadly Applicable Silencing Allele. *Neuron* **63,** 305–315 (2009).

92. Breslin, P. A., Spector, A. C. & Grill, H. J. Chorda tympani section decreases the cation specificity of depletion-induced sodium appetite in rats. *Am. J. Physiol.* **264,** R319-23 (1993).

93. Krashes, M. J. *et al.* Rapid, reversible activation of AgRP neurons drives feeding behavior in mice. *J. Clin. Invest.* **121,** 1424–8 (2011).

94. Geerling, J. C. & Loewy, A. D. Aldosterone-sensitive neurons in the nucleus of the solitary: efferent projections. *J. Comp. Neurol.* **498,** 223–50 (2006).

95. Geerling, J. C. *et al.* FoxP2 expression defines dorsolateral pontine neurons activated by sodium deprivation. *Brain Res.* **1375,** 19–27 (2011).

96. Menani, J. V, De Luca, L. A. & Johnson, A. K. Role of the lateral parabrachial nucleus in the control of sodium appetite. *Am. J. Physiol. Regul. Integr. Comp. Physiol.* **306,** R201-10 (2014).

97. Betley, J. N., Cao, Z. F. H., Ritola, K. D. & Sternson, S. M. Parallel, Redundant Circuit Organization for Homeostatic Control of Feeding Behavior. *Cell* **155,** 1337–1350 (2013).

98. Nation, H. L. *et al.* DREADD-induced activation of subfornical organ neurons stimulates thirst and salt appetite. *J. Neurophysiol.* **115,** 3123–9 (2016).

Online Methods

Animals. All experiments were approved by the Institutional Animals Care and Use Committee at the University of Washington. Heterozygous male and female *Hsd11b2*$^{Cre/+}$ or C57BL/6J (wild-type) mice were used for all experiments, ranging from 6-24 weeks. Animals from the same litter were split randomly between control and experimental groups, roughly half and half for each litter. Animals were group housed with littermates before and after stereotaxic surgery,

with *ad libitum* access to water and rodent diet (Picolab, number 5053) or a low-sodium diet (<0.02% NaCl, D99091603, Research Diets). During experiments they were individually housed with indicated food and water available *ad libitum* in a 12-h light/dark cycle (17:00-5:00) at ~22°C.

***Hsd11b2*$^{Cre:GFP}$ mice.** *Hsd11b2*$^{Cre:GFP}$ mice were made by inserting a 5.5 kb 5' arm and a 4.2 kb 3' arm into a targeting vector with ires-Cre:GFP, frt-flanked SV-Neo gene (for positive selection) and HSV-TK and *Pgk*-DTa genes (for negative selection). Each arm was made by PCR amplification (Phusion polymerase) from a mouse C57Bl/6 BAC clone with *Pac*1 and *Sal*1 sites at the ends of the 5' arm and *Pme*1 and *Not*1 sites at the ends of the 3' arm; both arms extend outward from a site just downstream of the endogenous termination codon of *Hsd11b2*. The targeting construct was electroporated in G4 (129/Sv x C57Bl/6 hybrid) embryonic stem cells. Correct gene targeting was detected in 28 of 71 clones by Southern blot using *Ssp*I and a ^{32}P-labeled probe outside the 5' arm. One of the clones gave high percentage chimeras and germline transmission. The SV-Neo gene was removed by a cross with *Gt(ROSA)26Sor-FLP recombinase* mice, and then *Hsd11b2*$^{Cre:GFP}$ mice (identified using a 3-primer PCR strategy) were continuously backcrossed to C57Bl/6 mice.

Viruses: AAV serotype 1 viruses (AAV1-Synapsin-DIO-hM3Dq:mCherry, AAV1-Efl1α-DIO-Synaptophysin:YFP, AAV1-Ef1α-DIO-mCherry, AAV1-Synapsin-DIO-hM4Di:mCherry, AAV1-Synapsin-DIO-YFP, AAV1-CBA-DIO-GFP:TetTox) were generated at the University of Washington as described[99]. AAV1 virus (420 nL) was injected at a titer of ~10^9 viral particles per microliter.

Stereotaxic Surgery. Mice (6-9 weeks old) were anesthetized with isoflurane and placed in a small-animal stereotax (Kopf Instruments). Coordinates for the anterior-posterior plane were normalized using a correction factor (F = Bregma-Lambda distance/4.21). Cre-dependent virus was bilaterally injected into the NTS (antero-posterior (AP), - 7.1 mm; medio-lateral (ML), ± 0.30 mm; dorso-ventral (DV), - 5.3 mm). Virus was bilaterally injected over 10 min for a final volume of 0.42 μL using glass capillaries and pressure injection (Nanoinject II, Drummond Scientific). Mice were given a minimum of two weeks of recovery before starting experimental manipulations. Animals that received viral injections that missed the target sight (no fluorophore visible) were excluded from analysis.

Sodium depletion. Animals were individually housed in BioDAQ recording chambers (Research Diets) and acclimated to a low-sodium diet, 0.5 M NaCl, and water available *ad libitium* for 3-5 days. Salt access was then removed, and mice were treated with two doses of 40 mg/kg furosemide, spaced 24 h apart; 24 h following the second injection, access to 0.5 M sodium-chloride was returned 20 min after the start of the dark cycle as described[31]. Real-time data were recorded by the BioDAQ over a 4-h period. Changes in intake are measured as grams, which were converted to and reported as mL (1 g H_20 or 0.5 M NaCl = 1 mL). For inhibition experiments (using hM4Di), CNO (1 mg/kg) was administered 40-50 min before access to 0.5 M NaCl was returned. For experiments looking at effects of sodium depletion on food intake, salt access was not returned until 2 h into the dark cycle, and food intake was recorded during this time.

Taste Tests. Mice were acclimated for 3-5 days in BioDAQ recording chambers, and all intake was monitored real-time using this system. Changes in intake are measured as grams, which were converted to and reported as mL (1 g H_20 and all tastants = 1 mL). Animals were given *ad libitum* access to 2-3 drinking bottles, one of which always contained water. Water intake was not monitored in the 3-bottle taste tests. After a minimum of one-day exposure to a new solution (to circumvent effects of neophobia), animals received 3 days of saline injections and baseline intake recordings before administering CNO (1 mg/kg) intraperitoneally 30-40 min before the start of the dark cycle on day 4. Baseline intake was recorded as the average of 3 days. In some cases, the BioDAQ recording system had errors and lost a night of data, and in these cases baseline intake was averaged from only 2 days. If data from the test night ("CNO") were lost, that animal was excluded from analysis for that tastant. Fluid intake was also recorded during the dark cycle and the following day to check for any long-term effects of HSD2 neuron activation on fluid intake ("Recovery"). Animals were kept on a low-sodium diet so that there was no alternative sodium source that could interfere with the taste tests. Individual animals underwent multiple taste tests, and the tastants were presented in different orders for different cohorts of mice to avoid effects of previous tasting experiences, although all mice were given NaCl in the first test. (**Fig 2b**). For experiments looking at changes in preference for high vs. low concentrations of NaCl, mice were given access to 0.5 M and 75 mM NaCl, with water available in the cage-top. On the night of recording, mice were given an injection of either saline or CNO 30-40 min before the start of the dark cycle, and water access was removed for the night. Each mouse received 2 days of saline and 2 days of CNO injections, with a minimum of 2-day recovery between injections. The preference and intake are an average of the 2 days of treatment.

Pharmacological injections. Pharmacological agents were administered intraperitoneally. CNO (1mg/kg; Tocris 49-361-0) was prepared in sterile 0.9% saline and stored at -20°C until use. Furosemide (Hospira) was stored at room temperature and administered at 40 mg/kg body weight.

Locomotion. Animals were placed in locomotion chambers (Columbus Instruments) from 9:00-13:00 for 3-d to acclimate to the cages. On day 4 and 5, mice were given 1.5 hours to acclimate, and then received an injection of saline one day and CNO (1 mg/kg) on the other. The order of injections was randomized between animals, and activity was recorded as beam-breaks by OptoMax software. Animals were returned to their home-cage each night. No food or water was available while mice were in the locomotion chambers. Mice that underwent locomotion studies were also used for the low vs. high salt experiments.

Histology. Mice were anesthetized with buprenorphine and perfused with 0.9% saline followed by 4% paraformaldehyde (PFA) in 0.1 M phosphate buffer (PB; pH=7.4). After an overnight post-fix in 4% PFA, brains were cryoprotected overnight in 30% sucrose before being embedded in OCT and stored at -80°C. Free-floating sections (30 μm) were collected on a cryostat. They underwent three washes in PBST (phosphate buffer saline + .03% Triton-X 100), and were blocked in 3% normal donkey serum in PBST (1-2 h). Sections were then incubated overnight at 4°C in primary antibody (sheep anti-Foxp2 1:2500 (AF5647, R&D Systems[100]), rabbit anti-c-Fos 1:2000 (#22505, Cell Signaling[101]), goat anti-c-Fos 1:300 (sc-52-G, Santa Cruz[102]), chicken anti-GFP 1:10,000 (ab13970, Abcam[103]) or rabbit anti-dsRed 1:1000 (No. 632496, ClonTech[104])). The next day, the tissue was washed three times in PBST and incubated 1-h in appropriate

secondary antibodies coupled to Alexa-Fluor 488/594 donkey anti-sheep, Alexa-Fluor 488/594 donkey anti-goat, Alexa Fluor 488/594 donkey anti-rabbit, or Cy5 donkey anti-goat (1:500; Jackson Immunoresearch Laboratories).

Imaging and cell counts. Images were acquired using an Olympus Fluoview FV1200 confocal microscope. For cell counts in the NTS and BNST, every third section underwent immunohistochemistry, was imaged and subsequently counted (90 μm apart). In the BNST, a circle was drawn around the HSD2-fiber terminals using ImageJ (when the channel containing Fos fluorescent immunoreactivity was not visible), and then Fos was counted inside and outside of that circle. For analysis of the PBN and pre-LC, tissue was collected 30 μm apart into 3 series, and 2 of those series underwent immunohistochemistry and was imaged (2/3 of the PBN and pre-LC was processed). The rostral-caudal level and subnuclei of the PBN was determined as described for Foxp2 immunoreactivity in the PBN in mice[100]. The location of the pre-LC was determined based on expression of Foxp2, as it is specific for this region[95]. Foxp2-immunoreactivity was always counted first to avoid bias from the presence of Fos when defining the mPBcl. Images were minimally processed to enhance brightness and contrast for optimal representation.

Statistics. Prism 6.0 (GraphPad Software) was used for all statistical analysis as outlined in **Supplementary Table 1-2**. Two-tailed, unpaired t-tests were used when comparing two data sets as indicated in the figure legends, and a Holm-Sidak post hoc test was used when analyzing cell counts where multiple, different regions were analyzed with tissue from the same mouse. Two-way ANOVA or repeated measures ANOVA were used with post-hoc Sidak multiple

comparisons tests, and one-way ANOVA paired with post hoc Tukey tests were used. Exact p-values for ANOVAs were calculated using a multiplicity adjusted p-value function in Prism. A *P* value of < 0.05 was considered statistically significant, and Excel was used to calculate exact *P* values that were < 0.0001 using appropriate information from Prism analysis (dF, t-ratio, etc). Data distribution was assumed to be normal but this was not formally tested. No statistical methods were used to pre-determine sample sizes but our sample sizes are similar to those reported in previous publications[31,105]. Error bars represent means ± s.e.m. All *n* values represent individual mice. The experimenter was not officially blinded to the experimental groups.

Code Availability: No code was written by the authors, and all analysis was done using Prism 6.0 (GraphPad Software) as provided by the manufacturer, or in some cases existing Excel functions were used to calculate exact *P* values for $P < 0.0001$. Data was stored within a project file for analysis.

Data Availability Statement: The data that support the findings of this study are available from the corresponding author upon request.

Methods-only References

99. Gore, B. B., Soden, M. E. & Zweifel, L. S. Manipulating gene expression in projection-specific neuronal populations using combinatorial viral approaches. *Curr. Protoc. Neurosci.* **4,** 4.35.1-4.35.20 (2013).

100. Geerling, J. C. *et al.* Genetic identity of thermosensory relay neurons in the lateral parabrachial nucleus. *Am. J. Physiol. Regul. Integr. Comp. Physiol.* **310,** R41-54 (2016).

101. Juan De Solis, A., Baquero, A. F., Bennett, C. M., Grove, K. L. & Zeltser, L. M. Postnatal undernutrition delays a key step in the maturation of hypothalamic feeding circuits. *Mol. Metab.* **5,** 198–209 (2016).

102. Ma, C.-W. *et al.* Postnatal expression of TrkB receptor in rat vestibular nuclear neurons responsive

to horizontal and vertical linear accelerations. *J. Comp. Neurol.* **521,** 612–625 (2013).

103. Enjin, A. *et al.* Identification of novel spinal cholinergic genetic subtypes disclose Chodl and Pitx2 as markers for fast motor neurons and partition cells. *J. Comp. Neurol.* **518,** 2284–2304 (2010).

104. Bochorishvili, G., Stornetta, R. L., Coates, M. B. & Guyenet, P. G. Pre-Bötzinger complex receives glutamatergic innervation from galaninergic and other retrotrapezoid nucleus neurons. *J. Comp. Neurol.* **520,** 1047–1061 (2012).

105. Rowland, N. E., Farnbauch, L. J. & Crews, E. C. Sodium deficiency and salt appetite in ICR: CD1 mice. *Physiol. Behav.* **80,** 629–35 (2004).

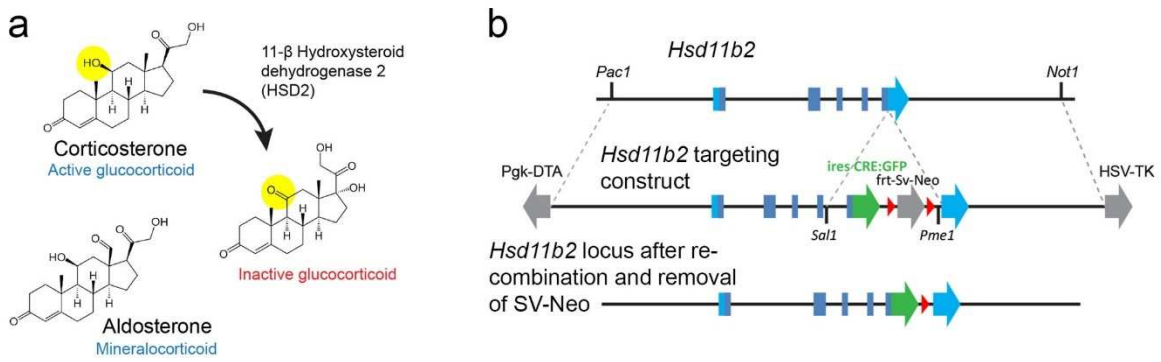

Supplementary Figure 1

Function of HSD2 and generation of *Hsd11b2*^{Cre} mice.

(**a**) HSD2 converts corticosterone to an inactive form that can no longer compete with aldosterone for the mineralocortioid receptor. (**b**) Diagram showing: top, the *Hsd11b2* gene (5 exons spanning ~5.5 kb with coding region in dark blue). Middle, the targeting vector; Bottom, *Hsd11b2* locus after recombination and removal of the frt-flanked SV-40 NeoR selection gene. Some key restriction enzyme sites used for cloning are shown. Diagram is not to scale.

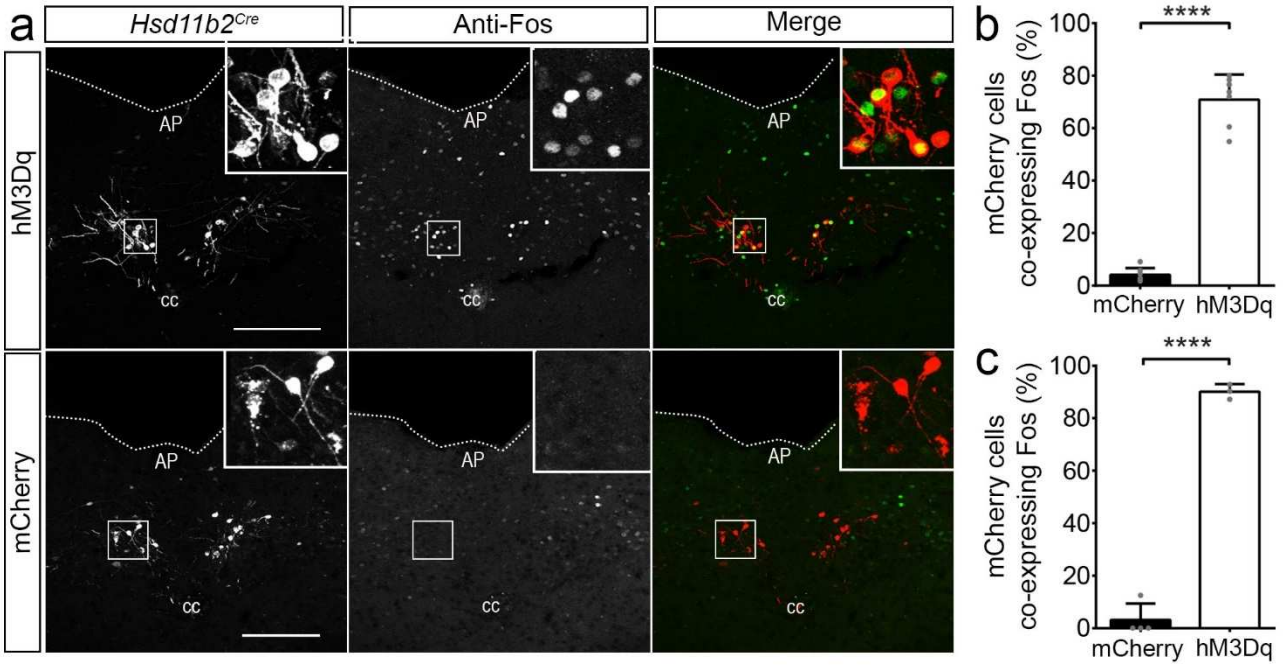

Supplementary Figure 2

CNO activates virally-targeted HSD2 neurons in the NTS.

(**a**) Representative sections from mCherry or hM3Dq:mCherry-transduced *Hsd11b2*^{Cre} animals following i.p. injection of CNO (1.0 mg/kg) and subsequent immunohistochemical staining for Fos. Scale bar, 200 µm. (**b, c**) Quantification of the percentage of mCherry-expressing neurons in the NTS co-expressing Fos in (**b**) male (n = 7 mice per group, two-tailed, unpaired t-test, *P* = 5.17E-10) and (**c**) female (n = 3 and 4 mice; two-tailed, unpaired t-test, *P* = 3.559E-06) *Hsd11b2*^{Cre} mice. AP, area postrema. cc, central canal.

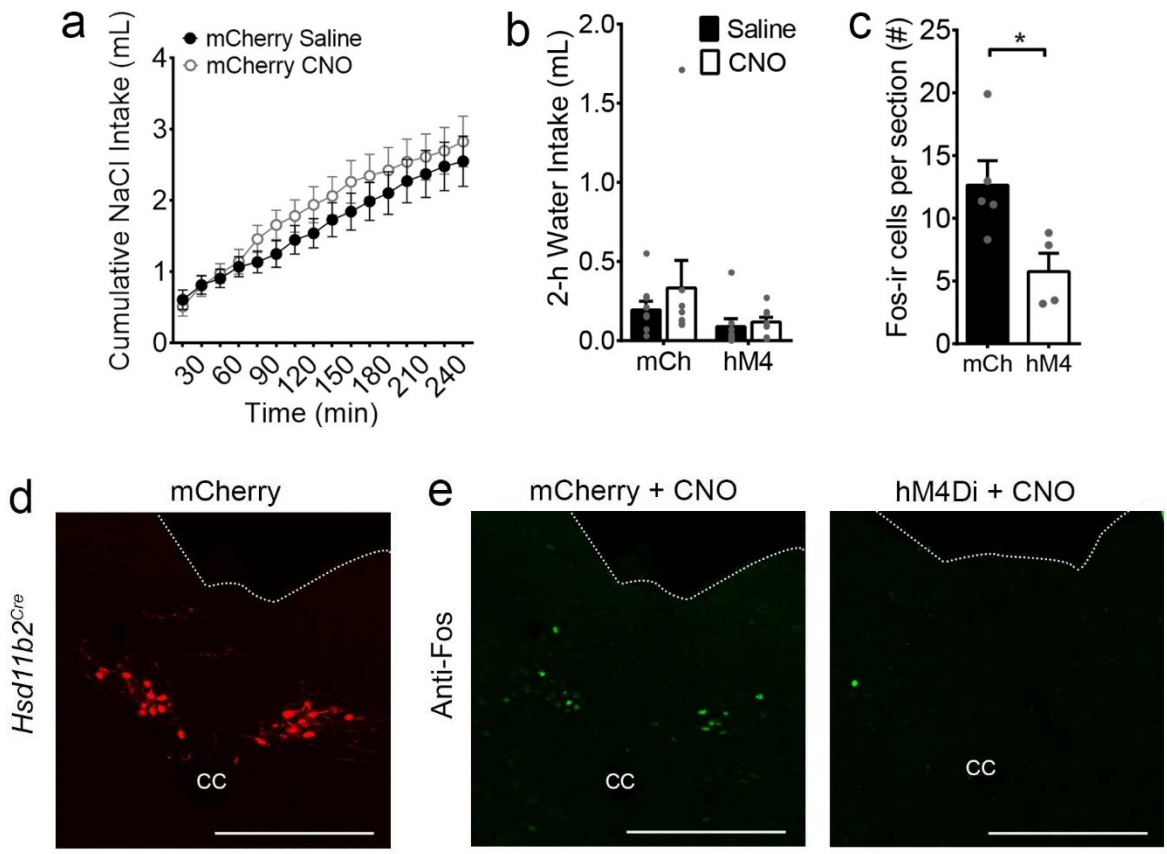

Supplementary Figure 3

Effects of hM4Di-mediated inhibition of HSD2 neurons.

(**a**) There was no change in sodium intake following sodium-depletion in *Hsd11b2*^{Cre} control mice expressing mCherry following injections of either saline or CNO (1mg/kg) (Repeated measure ANOVA, P = 0.382). (**b**) There was no change in water intake during the first 2-h after NaCl was returned to sodium depleted *Hsd11b2*^{Cre} mice expressing either mCherry or hM4Di:mCherry (paired salt intake data from from panel a and **Fig. 1f)** (Repeated measure ANOVA, P = 0.589). (**c**) CNO administration in sodium-depleted mice decreased Fos expression in the NTS of mice that expressed hM4Di:mCherry as compared to mCherry (unpaired, two-tailed t-test, P = 0.031). (**d**) Representative image showing mCherry fluorescence in HSD2 cells at the rostral-caudal level where Fos is shown in the panel e. (**e**) Representative image showing that CNO administration decreased Fos-immunoreactivity in the NTS of hM4Di:mCherry mice following sodium depletion, but no in mCherry controls. It was difficult to quantify HSD2 cell bodies in the hM4Di:mCherry-expressing mice, so Fos is not shown as a percentage of HSD2 neurons but rather represented as overall expression in the NTS. Scale bar, 100 µm. cc, central canal.

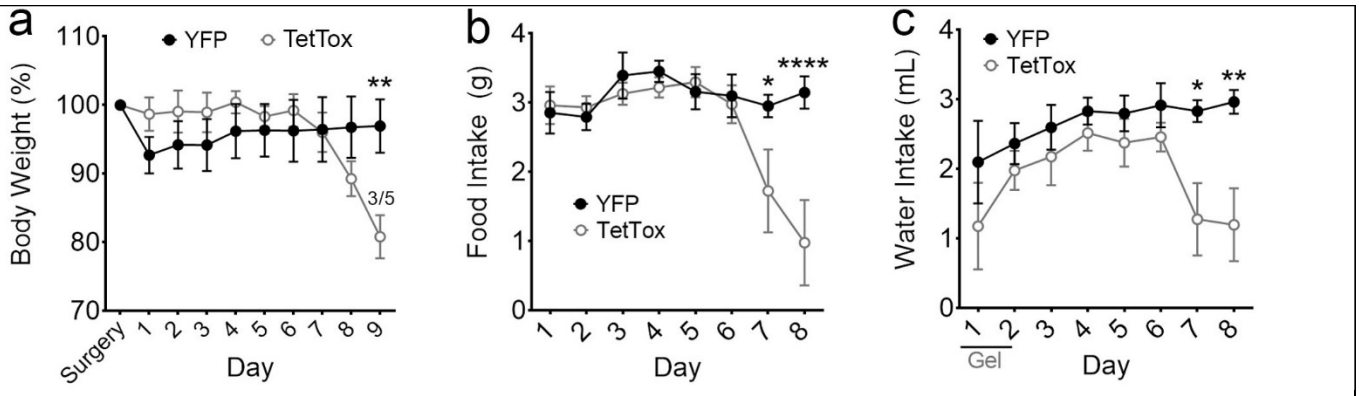

Supplementary Figure 4

Chronic inactivation of HSD2 neurons is fatal.

HSD2 neurons were targeted in the NTS with AAV-DIO-GFP:TetTox in a mix of male (n = 2) and female (n = 3) *Hsd11b2*^{Cre} mice. HSD2 neurons were transduced with AAV-DIO-YFP in control mice (male, n = 1; female, n = 5). (**a**) Mice became ungroomed (data not shown) and dropped to 80% of their pre-surgery body weight, at which point they were euthanized. On day 9, 3/5 mice were removed from the study (shown on graph), and the remaining 2/2 dropped to 80% and were euthanized on day 10 (Day 9, ** $P = 0.009$). (**b**) Overnight food (Day 7 * $P = 0.039$, day 8 **** $P < 0.0001$)(**c**) and water intake (Day 7 * $P = 0.028$, day 8 ** $P = 0.008$) both dropped the night before mice started to rapidly lose weight. Repeated measure ANOVA with post-hoc Sidak's multiple comparisons were used.

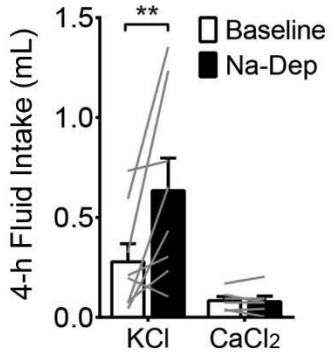

Supplementary Figure 5

Mice increased KCl consumption following sodium depletion.

Male wild-type mice increased their intake of 0.5 M KCl but not $CaCl_2$ following furosemide-induced sodium depletion (Repeated measures ANOVA, Sidak post hoc. KCl ** $P = 0.007$, CaCl2 $P = 0.999$). Some of these mice had undergone a bout of sodium depletion (with at least a week recovery time) prior to this test.

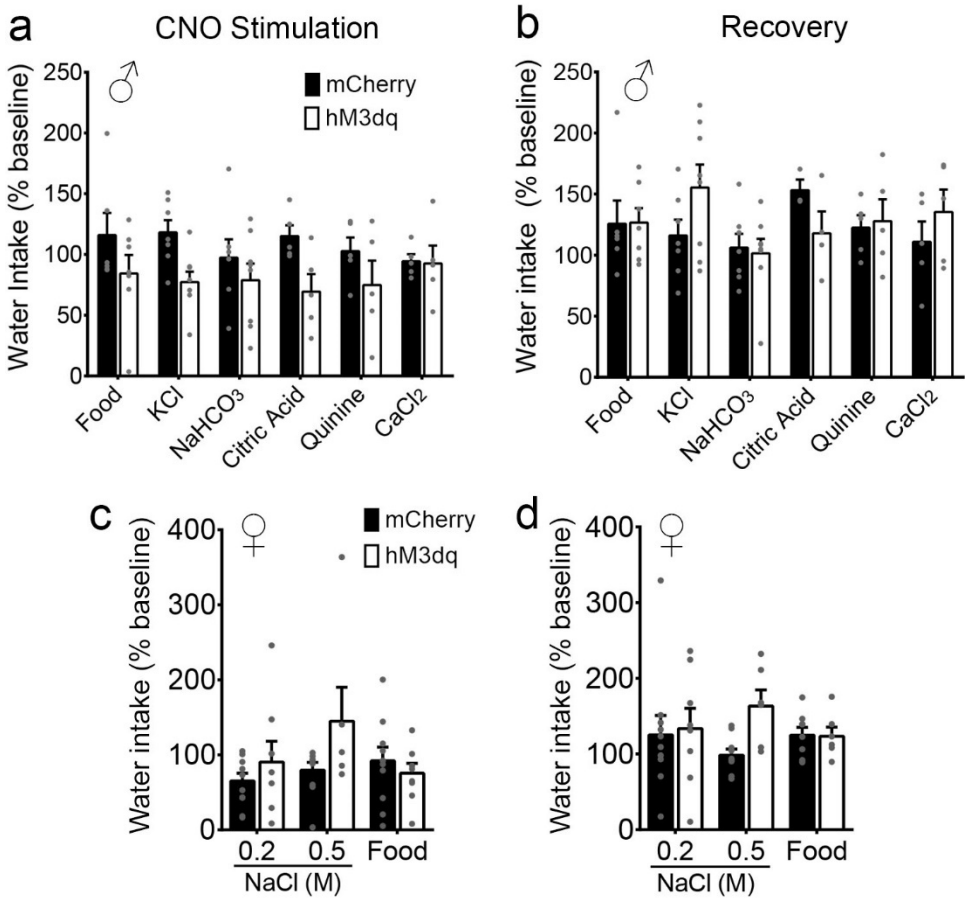

Supplementary Figure 6

Activation of HSD2 neurons does not alter water intake.

Water intake (4 h) expressed as a percentage of baseline intake from two-bottle choice assays in response to CNO (1 mg/kg) administration or the following night (Recovery). (**a, b**) Water intake in male mice from taste assays in **Fig. 2b** or paired with food intake from **Fig. 2d** (two-way ANOVA. CNO Stim, *P* = 0.6930. Recovery, *P* = 0.3293) Water intake is not shown from the sucrose taste test because mice predominantly drank sucrose instead of water, and water was not measured during the 3-bottle assay in **Fig. 2c**. (**c, d**) Water intake in female mice during the two-bottle choice tests shown in **Fig. 1c**, or paired with food intake from **Fig. 2d** (two-way ANOVA. CNO Stim, *P* = 0.1663. Recovery, P = 0.2376).

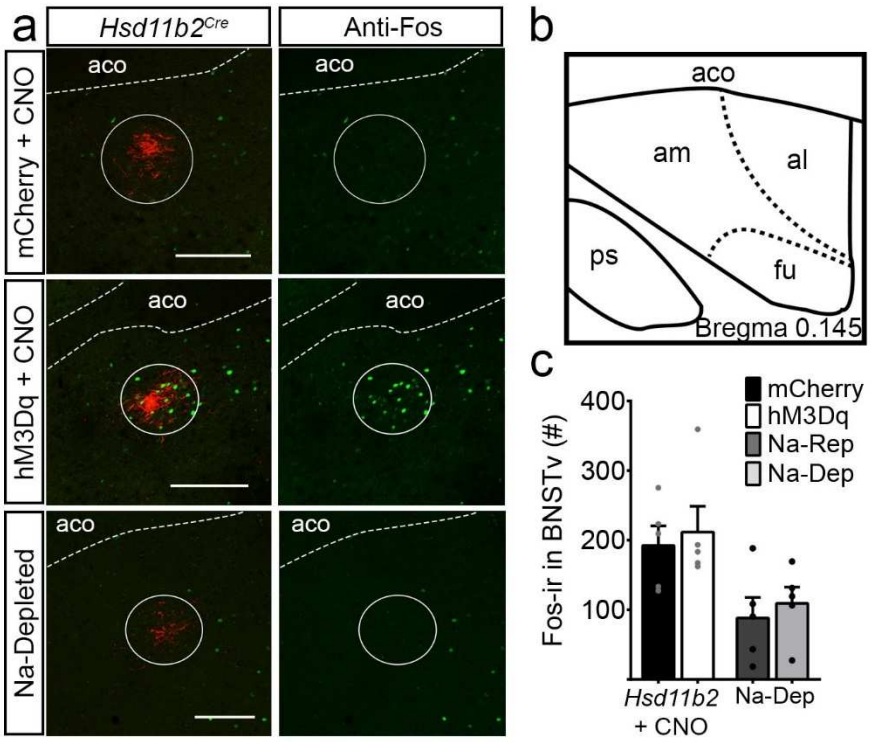

Supplementary Figure 7

Differential Fos induction in the BNSTv.

(**a**) Representative sections of immunoreactivity for Fos in the BNSTv of male mice with mCherry expressed in terminals of HSD2 neurons originating in the NTS. Scale bar, 60 µm. (**b**) Schematic showing anatomy of the ventral BNST. (**c**) A circle was drawn around fiber terminals, and Fos was counted within the circle (**Fig. 3d**), and (**c**) throughout the rest of the BNSTv. No changes in the number of Fos-immunoreactive cells were detected that were not directly under the fibers (multiple, two-tailed t-tests with Holm-Sidak post hoc. *Hsd11b2*, $P = 0.652$. Na-dep, $P = 0.626$). aco, anterior commissure; am, anteromedial; al, anterolateral; fu, fusiform; ps, parastrial nucleus.

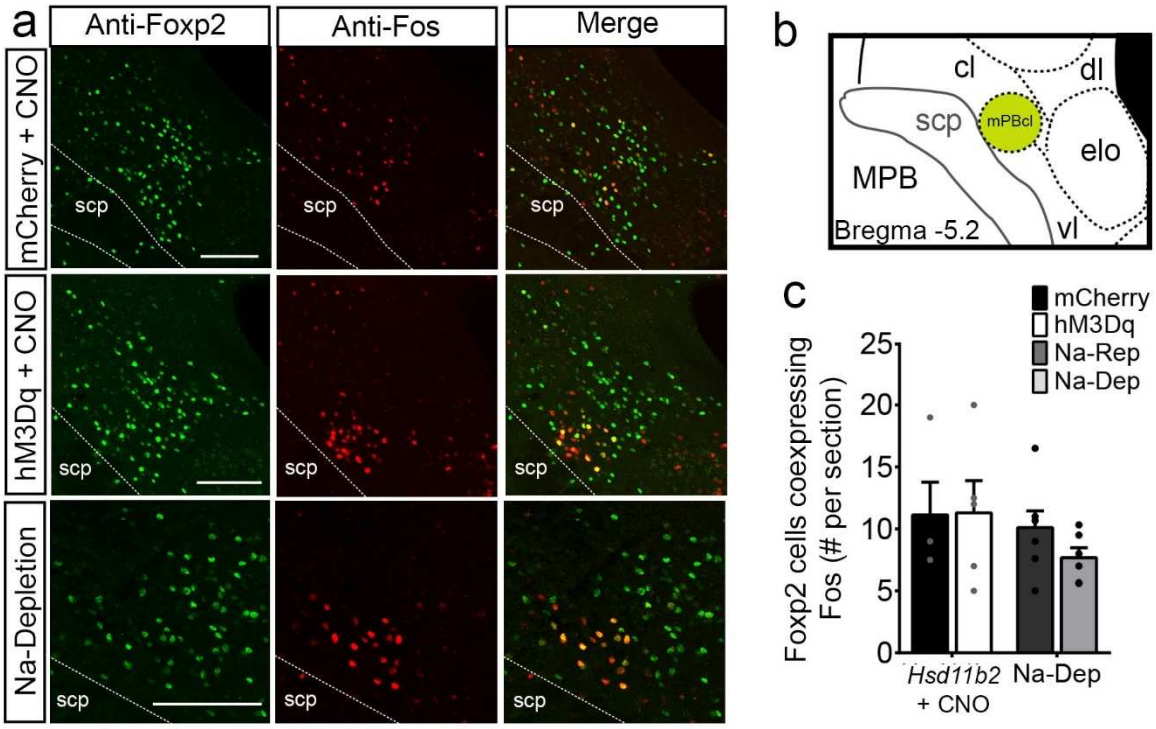

Supplementary Figure 8

Fos induction in the PBN.

(**a**) Representative images showing location of Foxp2 and Fos immunoreactivity in the mPBcl of the lateral parabrachial nucleus in response to sodium-depletion, or mCherry and hM3Dq:mCherry-expressing *Hsd11b2*^{Cre} mice in response to CNO. Scale bar, 60 µm. (**b**) Schematic showing relative location of neurons that co-express Foxp2 and Fos (yellow). (**c**) Quantification of neurons co-expressing Foxp2 and Fos in the rest of the central lateral (cl) and dorsal lateral (dl) region of the parabrachial nucleus in the same sections counted for **Fig 3b** (multiple, two-tailed t-tests with Holm-Sidak post hoc. *Hsd11b2*, P = 0.9510. Na-dep, P = 0.312). scp, superior cerebellar peduncle; vl, ventral lateral; elo, external lateral; MPB, medial parabrachial nucleus.

Chapter 3

Foxp2 neurons and the role of the PBN in salt appetite

*These are unpublished data

Introduction

Many brain regions have been implicated in the control of salt appetite, although the neural mechanisms still remain to be elucidated. The PBN has long been thought to have a role in salt appetite, and lesions of the parabrachial nucleus block or attenuate salt appetite[106,107]. It is unclear if these lesions disrupt sodium appetite itself or produce defects in gustatory processing[108], as the medial PBN is part of the ascending gustatory pathway[109]. However, the PBN and a nearby region called the pre-locus coeruleus (pre-LC), receive projections from aldosterone-sensitive, HSD2-expressing neurons in the hindbrain whose activation is sufficient to drive sodium appetite[59,110]. In addition, both sodium depletion and HSD2 neuron activation increases Fos expression in both the lateral PBN (LPBN) and pre-LC, specifically in neurons that express the transcription factor Foxp2[95,110]. Therefore, we hypothesized that activation of Foxp2 neurons in the LPBN and pre-LC would induce a sodium appetite similar to that induced by HSD2 neuron activation.

Results

To test our hypothesis, we generated a genetic knock-in mouse expressing Cre recombinase at the *Foxp2* locus[111] (*Foxp2*^{Cre}). Following injection of AAV1-DIO-YFP into the LPBN and pre-LC, the majority of cells expressing YFP were also Foxp2-immunoreactive (85.18±3.56%, n = 3). To determine whether Foxp2 neurons can drive sodium appetite, Foxp2 neurons were transduced with the modified G-protein coupled receptor hM3Dq fused to mCherry

(AAV1-DIO-hM3Dq:mCherry) and these neurons were activated using peripheral injections of the physiologically inert ligand for hM3Dq, clozapine-N-oxide (CNO; **Fig 1a**). All mice avoided intake of an aversive concentration of salt regardless of treatment with saline or CNO, indicating that Foxp2 neuron activation alone is insufficient to drive sodium intake (**Fig 1b**).

Given that many pharmacological manipulations of the PBN enhance sodium appetite but do not increase salt intake under normal conditions[96], it was also tested whether activation of Foxp2 neurons could drive sodium intake in a sodium-depleted state. Unexpectedly, CNO-induced activation of hM3Dq in Foxp2 neurons decreased intake of both water and 0.5 M NaCl during the first 4 h of the dark cycle, relative to mCherry-expressing control mice (**Fig 2a**). Further, while Foxp2-neuron activation did not significantly decrease normal water intake (baseline), it did significantly decrease water intake following overnight water deprivation (**Fig 2b**). In addition, there were no changes in food intake either under normal conditions (baseline) or following an overnight fast (**Fig 2c**), indicating that Foxp2-neuron activation specifically decreases fluid, but not food, intake.

The projection pattern of Foxp2 neurons in either the pre-LC or LPBN was examined by transducing either population with a virus driving expression of synaptophysin:YFP (AAV1-DIO-Synaptophysin:YFP; **Fig 3a-b**). Foxp2 neurons in the LPBN send clear projections to the medial preoptic area (MPO), the paraventricular nucleus (PVN), the paraventricular nucleus of the thalamus (PVT), the ventral-lateral periaqueductal gray (PAGvl), and ventral tegmental area (VTA; **Fig 3a**), with additional projections to the dorsal media hypothalamus (DMH), parasubthalamic nucleus and throughout the rostral-caudal extent of the lateral hypothalamic area (LHA). Foxp2 neurons in the pre-LC had a similar but distinct projection pattern, with projections to the DMH, arcuate nucleus (ARC), LHA, ventral bed nucleus of the stria terminalis

(BNSTv), and NTS (**Fig 3b**). Weaker projections were observed to the PVH, VTA, PVT, PAG, and central medial thalamus. It is important to note that the targeting of synaptophysin to the pre-LC also included some cells in the medial PBN. Overall, the projections of the Foxp2 neurons from either nucleus reported here are similar to what has been previously described[112].

Discussion

These data demonstrated that activation of Foxp2 neurons in the LPBN and pre-LC is not sufficient to induce salt appetite, but instead appears to have a mildly inhibitory role on sodium intake following sodium deprivation. However, it is unclear whether this decrease was due to general inhibition of intake of all fluids. Activation of Foxp2 neurons also decreased water intake in a dehydrated state but not food intake regardless of hunger state. These findings are surprising since some of these neurons are likely direct downstream targets of HSD2 neurons, which potently drive sodium intake without affecting water consumption[59,110]. However, Foxp2 is expressed throughout most subnuclei of the PBN, with the exception of the external lateral PBN[100,113]. One possibility is that Foxp2 is also expressed in a population of oxytocin-receptor (Oxtr) expressing neurons in the LPBN, which have recently been implicated in the regulation of thirst and salt intake[114]. However, this seems unlikely because the projection patterns of the Oxtr-neurons are distinct from Foxp2 neurons; Oxtr-neurons innervate the dorsal BNST and central amygdala[114], while Foxp2 neurons do not (**Fig 3**). Therefore, the decrease in water and salt intake following PBN/pre-LC Foxp2 neuron stimulation is likely driven by a population of Foxp2 neurons that is distinct from both the Oxtr-expressing neurons and those that receive direct projections from HSD2 neurons. Foxp2 may also label additional functional cell populations, including those involved in cardiovascular regulation[113], respiration[115], and thermoregulation[100] (also see **Appendix I**).

In addition to being a part of the HSD2 salt-appetite promoting circuit, the LPBN is also thought to chronically inhibit sodium intake. In the rat, a number of pharmacological manipulations that suppress signaling within the LPBN[116–118], such as direct infusions of agonists for μ-opioid receptors[117,119], GABA receptors[120–122], α2-adrenergic receptor[61,116,122,123], or serotonin receptor antagonist[124,125], strongly promote or enhance salt and water intake. Presumably under normal conditions, the neurons targeted by these manipulations are signaling sodium satiety, or an alert that too much sodium has been consumed. Further evidence for this comes from a study showing that acute aldosterone infusion in the 4th ventricle and serotonergic or noradrenergic manipulation of the LPBN has a synergistic effect on sodium consumption[61]. The pharmacological infusions into the LPBN appear to be disinhibiting a break on sodium intake, allowing aldosterone (presumably signaling through HSD2 neurons) to more effectively drive sodium appetite. This complicates our interpretation of the effects of Foxp2 neuronal activation, because we may be simultaneously activating two functionally opposed circuits. It remains unclear whether the population of neurons that inhibits sodium intake also expresses Foxp2. Regardless, more specific markers are needed to further define how the PBN regulates sodium intake.

A more direct way to examine the role of the PBN in promoting salt appetite is to optogenetically activate terminals from HSD2 neurons in the PBN. Unexpectedly, but in agreement with findings described above, no increase in salt intake occurred following stimulation of HSD2 terminals in the PBN[59]. It is unclear whether the HSD2→PBN terminal activation also included projections to the pre-LC, so it is difficult to say whether this region can promote salt appetite. However, HSD2 neurons also project to the ventral BNST, and activation of these terminals can elicit sodium intake when paired with water deprivation. While BNST

lesions strongly attenuate sodium appetite[126–128], sodium depletion does not reliably induce Fos-immunoreactivity in this region[56,110] (but see Matsuda et al.[36]), and no genetic marker for their HSD2-neuron target cells has been identified. Altogether, these data suggest that the PBN may not actually promote sodium consumption and much remains to be elucidated about the neural circuitry downstream of HSD2 neurons.

PBN and pre-LC Foxp2 neurons send extensive projections throughout the brain, including many regions that have been implicated in salt-appetite behavior[112]. One specific projection of note is to the VTA; one paper showed that dopamine is released in the nucleus accumbens in response to consumption of salt, but only during sodium deficieny[20]. The study further suggested that this effect may be mediated via projections from Foxp2 PBN and pre-LC neurons to the VTA. It is therefore possible that the PBN and pre-LC Foxp2 neurons could be involved in the increase in palatability of high concentrations of sodium following sodium depletion[11], but alone cannot generate motivated sodium consumption[59]. However, other studies show that optogenetic inhibition of the ventral pallidum selectively disrupts salt seeking while leaving consumption intact[28], but also may be important overall for tracking changes in taste value[24], suggesting that the Foxp2 neurons could be more important for motivation to seek out salt.

Overall, the role of Foxp2 neurons remains unclear, and more broadly, the roles of the PBN and pre-LC need to be disentangled. A more specific genetic marker for the population of Foxp2 neurons that receive HSD2 input will likely be critical in this pursuit. However, given that activation of HSD2→PBN terminals is not sufficient to induce sodium intake, it seems likely that these nuclei will be involved in a subtler aspect of sodium appetite, such as the shift in the

palatability of sodium following sodium depletion, or perhaps another unidentified function of the HSD2 neuronal circuit altogether.

Figures:

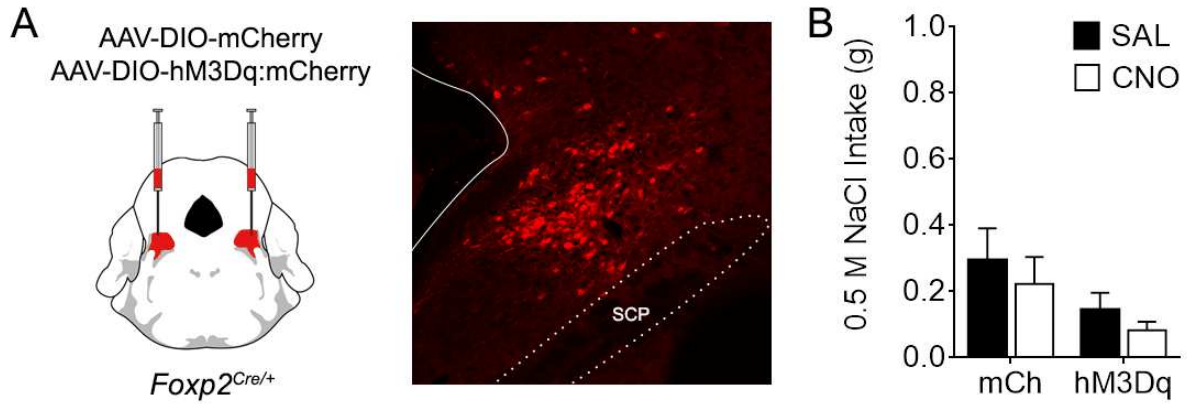

Figure 1: Chemogenetic activation of Foxp2 neurons is not sufficient to increase sodium intake.

(A) Stereotaxic delivery of Cre-dependent hM3Dq:mCherry (hM3Dq) or mCherry (mCh) into the PBN and pre-LC of *Foxp2*$^{Cre/+}$ mice. SCP, superior cerebellar peduncle. (B) No difference in intake of NaCl in two-bottle choice tests for water or NaCl during the first 4 h of the dark cycle in response to intraperitoneal injection of saline (SAL) or CNO. (n= 7 hM3Dq, 9 mCh; Two-way ANOVA; interaction $F(1,14) = 0.04588$, $P = 0.8335$)

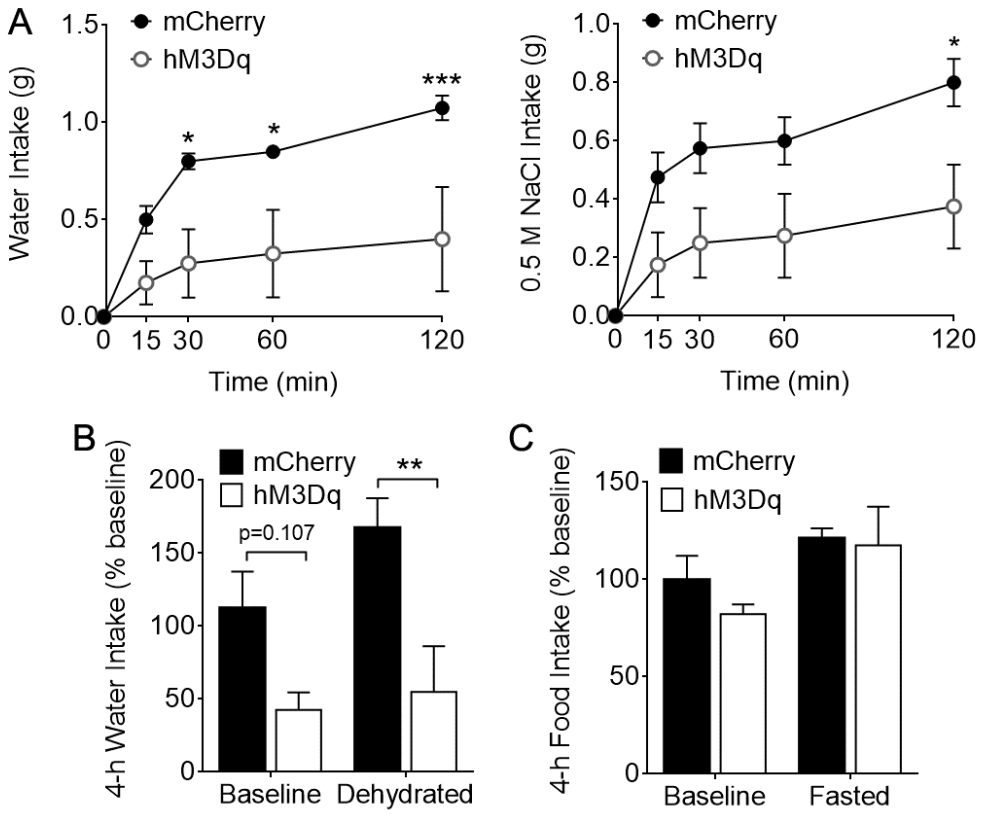

Figure 2: Foxp2 neuron activation decreases fluid intake during deprivation states.

(A) CNO activation of hM3Dq-expressing Foxp2 neurons caused mice to drink less of both water and NaCl following furosemide-induced sodium deprivation compared to mice expressing mCherry. (n = 4/group; two-way RM ANOVA; *post hoc* Sidak's multiple comparisons test; water: interaction F(4, 24) = 5.029, P = 0.0043, NaCl: interaction F(2,24) = 5.020, P = 0.0044). (B) Mice expressing hM3Dq did not drink significantly less water during the first 4 h of the dark cycle following CNO-stimulation compared to mCherry control mice (baseline), although they did drink less following overnight water deprivation. (n = 4/group; two-way RM ANOVA; *post hoc* Sidak's multiple comparisons test; interaction F(1,6) = 1.795, P = 0.2288). (C) No difference in food intake following CNO-stimulation either during the first 4 h of the dark cycle (baseline) or following an overnight fast. (mCherry n = 4, hM3Dq n = 4; two-way RM ANOVA; *post hoc*

Sidak's multiple comparisons test; interaction F(1,5) = 0.4654, P = 0.4654) * P < .05, **P < .01 *** P < .001

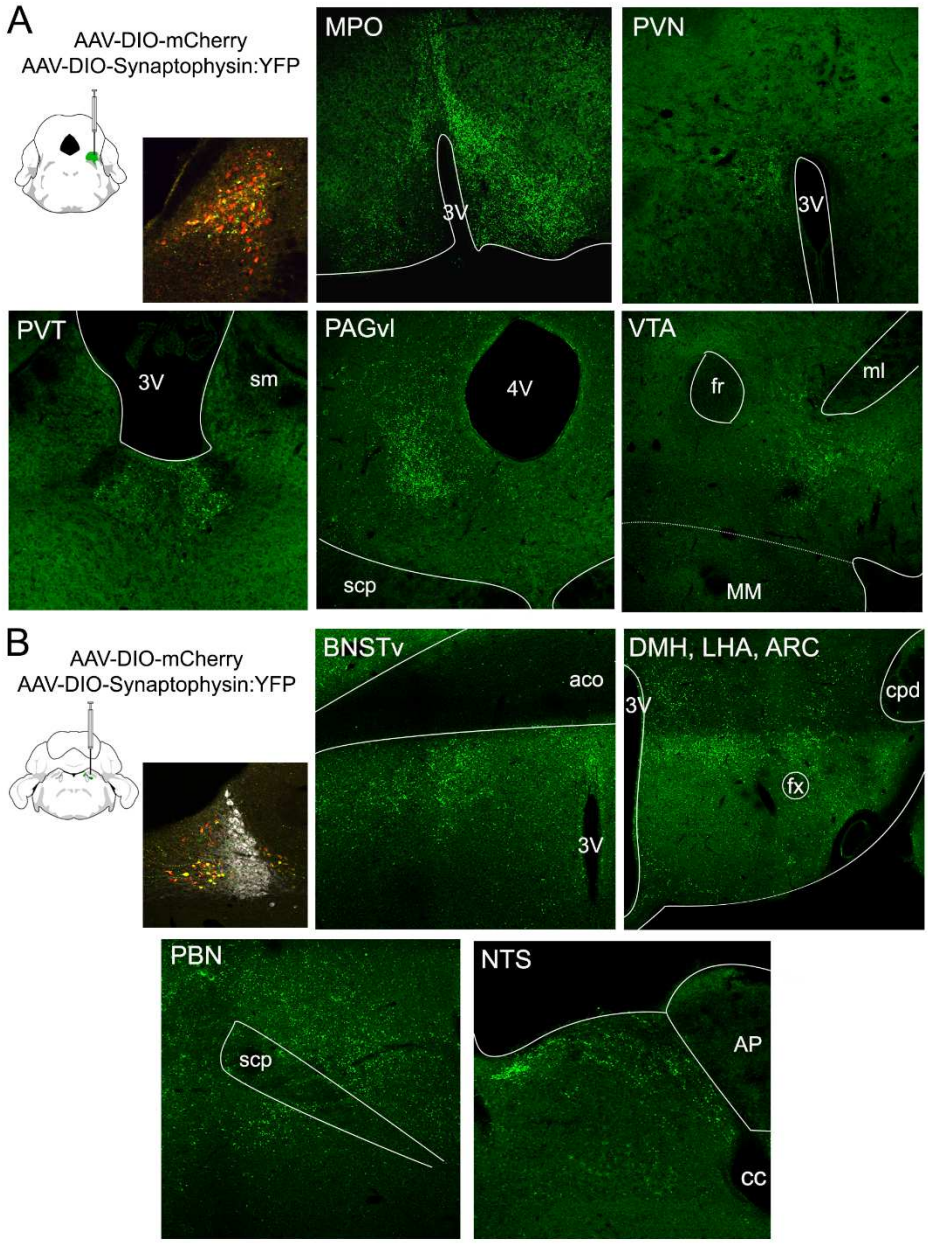

Figure 3: Downstream projections of Foxp2 neurons in the pre-LC and PBN.

Stereotaxic delivery of Cre-dependent synaptophysin:YFP and mCherry in *Foxp2*$^{cre/+}$ mice into either the (A) LPBN or (B) pre-LC in order to identify downstream terminal fields. MPO, medial preoptic nucleus; PVN, paraventricular nucleus; 3V, third ventricle; PVT, paraventricular thalamus; sm, stria medullaris; PAGvl, ventral lateral periaqueductal gray; scp, superior cerebellar peduncle; 4V, fourth ventricle; VTA, ventral tegmental area; fr,fascuculus retroflexus; ml, medial lemniscus; MM, medial mammillary nucleus; BNSTvl, ventral lateral bed nucleus of the stria terminalis; aco, anterior commissure; DMH, dorsomedial hypothalamis nucleus; LHA, lateral hypothalamic nucleus; ARC, arcuate nucleus; fx, fornix; cpd, cerebellar peduncle; NTS, nucleus of the solitary tract; AP, area postrema; cc, central canal.

Methods

All of the methods are identical to those described in Chapter 2.

Foxp2$^{\mathbf{Cre:GFP}}$: *Foxp2*$^{Cre:GFP}$ mice were made by inserting a 9 kb 5' arm and a 5 kb 3' arm into a targeting vector with ires-Cre:GFP, frt-flanked SV-Neo gene (for positive selection) and HSV-TK and *Pgk*-DTa genes (for negative selection). Each arm was made by PCR amplification from a mouse C57Bl/6 BAC clone with *Pml*1 and *Sal*1 sites at the ends of the 5' arm and *Xho*1 and *Not*1 sites at the ends of the 3' arm; both arms extend outward from a site just downstream of the endogenous termination codon of *Foxp2*. The targeting construct was electroporated in G4 (129/Sv x C57Bl/6 hybrid) embryonic stem cells. Correct gene targeting was detected in 62 of 83 clones analyzed by Southern blot using *Stu*I and a^{32}P-labeled probe outside the 5' arm. One of the clones gave high percentage chimeras and germline transmission. The SV-Neo gene was removed by a cross with *Gt(ROSA)26Sor-FLP recombinase* mice, and then *Foxp2*$^{Cre:GFP}$ mice (identified using a 3-primer PCR strategy) were continuously backcrossed to C57Bl/6 mice

Chapter 4

Discussion and Future Directions

Summary

Our study was the first to show that HSD2 neurons are both necessary and sufficient for sodium appetite, and an important part of the neural circuitry that controls sodium homeostasis. We confirmed their major downstream projections to an unknown neuronal population in the BNSTv and to Foxp2 neurons in the PBN/pre-LC. We further demonstrated that activation of Foxp2 neurons is not sufficient to induce sodium intake, but activation of this previously undefined population of neurons can control water intake. Future studies with more specific genetic markers will be needed to further elucidate the role of the PBN and pre-LC in fluid homeostasis. A graphical summary of the neurons and regions discussed throughout this chapter and thought to be involved in sodium appetite is provided in **Figure 1**.

Discussion and Future Directions

In our hands, chronic inactivation of HSD2 neurons was lethal and rapidly elicited a drastic drop in body weight and overall health. Interestingly, when Resch et al. [59] chronically inactivated HSD2 neurons, they did not observe adverse effects on the overall health of the animals. They showed that inactivation of HSD2 neurons blocked sodium appetite, which is in agreement with our transient inactivation studies using the inhibitory DREADD, hM4Di. Thus, the morbidity reported in our paper is unlikely to be due to inactivation of the HSD2 neuronal population that drives sodium appetite. It is possible that that our inactivation experiments included an additional HSD2-expressing population that was not visible in the sections we examined for histological verification of viral targeting. Altogether, these data suggest that

HSD2 neurons in the NTS are necessary for sodium appetite but are unlikely to have an additional role that is necessary for immediate survival.

Our main finding that HSD2 neurons are sufficient to drive sodium appetite was replicated and extended by Resch et al[59]. The data from our lab looked solely at cumulative intake in the home cage during the dark cycle when mice are normally drinking[110]. The greater granularity of the experiments done by Resch et al. revealed an unexpected time course of HSD2 neuron activation driving sodium appetite. Their studies showed that HSD2 neuron stimulation under these same conditions resulted in a gradual increase in sodium intake across the duration of the stimulation, rather than rapidly inducing sodium intake following the presentation of salt[59]. However, mice will not increase their intake of sodium in response to HSD2-neuron activation when placed in a test cage during the day, unless they are also water deprived. In this second paradigm, the rapid increase in sodium consumption following HSD2 neuron activation requires Ang II signaling, as co-injection of an Ang II antagonist blocked sodium intake, while co-treatment with both Ang II and CNO increased licking for NaCl above that seen with treatment of either Ang II or CNO alone[59]. Resch et al. further showed that the slower intake observed using our protocol was not dependent on Ang II signaling, suggesting that there may be multiple mechanisms driving rapid versus sustained intake of sodium following sodium depletion. Alternatively, there may be an additional signal other than Ang II that is permissive to HSD2-induced sodium intake that is present at a circadian time-point that we caught during the start of the dark cycle but is absent during the day.

Ang II and aldosterone have long been reported to have a synergistic effect on sodium appetite[35,129], although the neural mechanisms have remained unclear. Given that HSD2-neurons respond to aldosterone[43,130], induce robust sodium consumption[59,110], and their activation

combined with Ang II administration leads to enhanced sodium appetite[35], their critical role in mineralocorticoid-induced salt appetite is well-established. However, HSD2 neurons still express Fos following adrenalectomy, where the resulting sodium appetite is due to loss of sodium reabsorption in the kidney as a result of complete loss of mineralocorticoid signaling[131]. This sodium appetite is reliant at least in part on Ang II[132,133], as global knock out of the Ang II receptor abolishes sodium intake following sodium-deprivation and other manipulations that typically result in increased sodium intake[36]. Interestingly, HSD2 neurons also express functional Ang II receptors that not only increase the firing rate of these neurons in acute electrophysiological slice recordings, but will further increase the firing rate of HSD2 neurons when paired with chronic administration of aldosterone[51,59]. Therefore, the synergistic effects of aldosterone and Ang II may be mediated at least in part by integration of these two peripheral signals in HSD2 neurons, although it remains to be determined whether increasing firing frequency of HSD2 neurons corresponds to increasing volumes of sodium intake.

In addition to the HSD2 neurons in the NTS, the subfornical organ (SFO) has been shown to have a large role in the regulation of sodium appetite, particularly in response to Ang II. Lesions of the SFO can block or attenuate sodium appetite[134], but not under all circumstances (e.g. does not block sodium intake following an adrenalectomy[135]). Loss of Ang II-receptors specifically within the SFO also severely attenuates sodium appetite[36], meaning that Ang II signaling in HSD2 neurons alone does not fully explain the role of Ang II in salt appetite. Additionally, chemogenetic or optogenetic stimulation of neurons in the SFO can drive both water and sodium intake[36,136]. Furthermore, optogenetic activation or inhibition of glutamatergic neurons in the SFO that project to the BNSTv can either increase or decrease sodium intake, respectively[36]. Activation of the BNSTv-projecting SFO neurons did not alter water intake,

directly contrasting with manipulation of other regions that receive projections from the SFO (OVLT and MnPO), which alter water but not salt intake[36,137]. Using slice electrophysiology, Matsuda et al. [36] confirmed that SFO→BNSTv neurons respond to Ang II and receive inhibitory input from local GABAergic neurons, which in turn are activated in response to increasing levels of salt present in the plasma and CSF. The activity of GABAergic neurons is controlled by the Na_x channel, which is expressed on glial cells in the SFO[138–140]. The proposed model is that when Ang II is elevated (dehydration, hypovolemia, hyponatremia), it binds to receptors in the SFO that are expressed on two functionally distinct populations, the water-promoting neurons (those that project to the OVLT and MnPO) and salt-promoting neurons (those that project to the

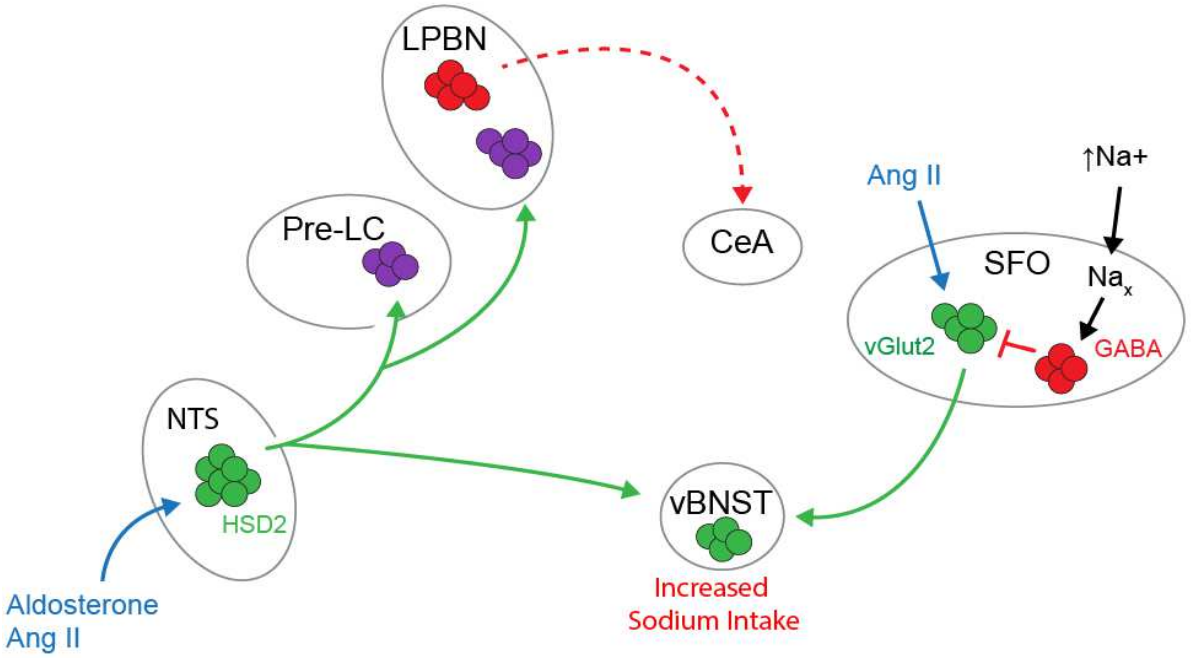

Figure 1: A graphical summary of the research summarized in Chapter 3 and Chapter 4 about the different nuclei and cells types known to be implicated in sodium appetite. The HSD2 neurons in the NTS project to the vBNST, and this projections is sufficient to increase sodium intake. Tis region also receives inputs from glutamatergic neurons in the SFO. A population of GABAergic neurons in the SFO works to counteract sodium intake when Nax channels detect high concentrations of sodium in the cerebral spinal fluid. HSD2 neurons putatively project to Foxp2-expressing neurons in the PBN and pre-LC, although the precise role fo these neurons in sodium appetite have not been identified. There is also a population of neurons that potently inhibit sodium appetite in the PBN, which is dependent on the CeA.

BNSTv). The salt promoting population is inhibited under conditions of increased sodium in body fluids[36], neatly providing a mechanism by which the SFO can control water and sodium intake depending on an animal's state of need, which is independent of HSD2 neurons in the NTS.

There is growing evidence to suggest that the BNSTv is an important nucleus and potential point of convergence for circuits controlling sodium appetite. In addition to the study mentioned above showing that neurons projecting from the SFO to the BNSTv are necessary and sufficient for sodium appetite[36], it has also been shown that optogenetic stimulation of the HSD2 terminals in the BNSTv can drive sodium intake[59]. The effects of HSD2 terminal stimulation have only been tested in water-deprived mice, and the rapid increase in sodium intake is likely dependent on the presence of Ang II, similar to what was seen with activation in cell bodies[59]. It therefore seems likely that the input into the BNSTv from the SFO is signaling the presence of Ang II, which can be integrated with input from the HSD2 neurons, allowing the BNSTv to be the primary site where the synergistic effects of Ang II and aldosterone occur. This region of the BNST also receives strong input from A1 and A2 adrenergic neurons in the medulla[94], which may contribute to the sodium consumption that occurs following injections of the a2-adrenergic antagonist yohimbine[141], which is dependent on an intact BNST[128]. Curiously, HSD2 neuron terminals in the BNSTv also overlap strongly with projections from AgRP neurons in the ARC, CGRP-expressing neurons in the PBN[51,59], and likely Foxp2 neurons in the pre-LC (see Chapter 3). Stimulation of AgRP terminals in the BNSTv increases food intake[97], and stimulation of CGRP terminals causes anorexia, although CGRP terminals are also more widely spread across the BNST[142]. The area of innervation by HSD2 terminals is very spatially restricted, and so it will be interesting to determine whether the neurons that receive input from the NTS also receive

input from these other regions, although functionally it seems like there must be some differences. Generally, this region of the BNST receives input from multiple neuronal populations carrying interoceptive information (sodium balance, visceral malaise, nutritional state, etc). However, the genetic identity of the neuronal populations in the BNST that receive this input to regulate sodium intake, as well as these other behaviors, is unknown and identifying markers will be an essential step needed to clarify how this region of the brain coordinates information.

The other major downstream target of HSD2 neurons is Foxp2-expressing neurons in the PBN and pre-LC, although the role of these neurons in salt appetite or in mediating other HSD2 neuron functions remains to be determined. Activation of HSD2 terminals in the PBN[59], as well as chemogenetic activation of Foxp2 neurons in the PBN/pre-LC, are insufficient to induce sodium intake (see Chapter 3). As in the BNSTv, AgRP neuronal terminals are intermingled with HSD2 terminals in both the pre-LC and PBN[51]. Given that chemogenetic activation of HSD2 neurons also has an anorexic effect provided the food is not salty[59,110], it seems likely that projections to either the BNSTv or PBN/pre-LC are mediating this anorexia. This anorexia is likely to be a similar phenomenon to that seen with AgRP-neuron stimulation, where activity of these neurons (or hunger) can suppress or override innate responses to stress, fear and pain in order to prioritize the behavioral output that promotes survival (feeding or foraging)[143–145]. However, it seems unlikely that the PBN/pre-LC projection in responsible for the HSD2-neurons induced anorexia given that no changes in food intake occurred following activation of Foxp2 neurons (see Chapter 3). This could still be due to Foxp2 being too broad of a marker to use for functional studies in the PBN/pre-LC. Additionally, a recent paper described additional, weaker projections of HSD2 neurons to the PVH, CeA, LHA, PSTN, VTA, and PAGvl that have not

been reported previously[51]. More work needs to be done to functionally map out the next nodes in the neural circuitry downstream of HSD2 neurons.

The location where the shift to an increased preference for salt during a sodium deficit is encoded in the brain is poorly understood. This question is complicated because the value of salt can be differentially regulated from the motivation to consume salt. Therefore, studies that look solely at intake of sodium cannot necessarily comment on whether the palatability of sodium changed without also looking for changes in behaviors like taste reactivity. However, it is unclear whether motivation to consume salt without an accompanying alteration in sodium palatability can supersede the aversive nature of salt, and whether animals would still consume the same amount of an aversive sodium solution. This can be dissociated in the opposite direction; lesions of the central nucleus of the amygdala decrease sodium intake following sodium depletion, but rats still demonstrate an increase in palatability in response to the taste of sodium[146]. Whether HSD2 neuron activation can induce a change in taste reactivity in response to sodium, or alternatively whether inhibition could block a change in taste reactivity, has not been demonstrated. Given that mice selectively increase their preference for a higher concentration of sodium compared to a lower concentration when given a choice between the two following HSD2 neuron activation, it does seem likely that there are changes in palatability of sodium associated with HSD2 neuron activity[110].

The regions that have been implicated as having a role in the change in value of sodium include the lateral hypothalamus, nucleus accumbens (NAc), and ventral pallidum (VP)[23,24,31,147]. Dopamine is released in the NAc in response to sodium following sodium depletion, and there are various changes in neural firing patterns, dendritic morphology, Fos, and gene expression[20,21,147–150]. However, pharmacological inhibition of the NAc shell does not alter

sodium appetite or the associated changes in sodium palatability, although rats did decrease their sucrose consumption[151]. Similarly, there are clear changes in activity in the VP in response to salt during sodium depletion[23], but optogenetic inhibition experiments in rats had no effect on cues associated with salt or sodium consumption[28]. However, these inhibition experiments targeted the anterior VP, whereas more posterior regions have been implicated as the important site for the assignment of valence[24,26,27]. In the lateral hypothalamus, neurons expressing the dopamine receptor D1R are essential for sodium appetite, although lesions of this region to do not appear to influence hedonic value of tastes[24,31]. All of these areas do appear to have some role in sodium appetite, although the precise nature of their involvement and how that relates to the known circuitry of HSD2 and SFO neurons needs to be further explored.

HSD2 neurons may also be involved in a wider variety of behavior and physiology than just the regulation of sodium intake during a state of sodium deficit. One obvious hypothesis is that the HSD2 neurons have a role in cardiovascular regulation, given that mineralocorticoids infused intracerebroventricularly can induce hypertension and reduce baroreflex sensitivity[152–154]. Supporting this possibility, one study has shown that brain-specific HSD2 deficiency, which would cause chronic activation of these neurons by glucocorticoids binding to mineralocorticoid receptors, results in both hypertension and an impaired baroreflex[49]. While activation of HSD2 neurons does not appear to affect blood pressure or heart rate[59], it remains possible that they have a more subtle effect related to the baroreflex rather than overt effects on blood pressure regulation. Another possibility is that HSD2 neurons regulate daily intake of sodium, independent of sodium need. Regulation of the lower, appetitive concentration of salt has often been proposed to be independent from the salt-appetite circuitry, although definitive testing has not been done to prove this. For example, it would be interesting to test whether inactivation of

HSD2 neurons can shift a sodium taste curve, which would imply that HSD2 neurons either impinge on salt-taste processing, or that the normal drive to consume appetitive salt is also mediated by HSD2 neurons. Determining whether HSD2 neurons can influence normal salt intake could be of particular importance, as humans tend to consume sodium in excess, and a study in 2010 attributed 1.65 million cardiovascular-related deaths to overconsumption of sodium[76]. Other studies have suggested that salt intake leads to overconsumption of both calories and dietary fat[155], and that obese patients have increased consumption and liking scores for salt[156,157]. In addition, both sodium depletion and treatment with mineralocorticoids causes hedonic deficits in behavior such as sucrose preference and working for rewarding stimulation of the LH[158–160], as well as increased anxiety and depressive phenotypes[161,162]. It would, therefore, be prudent to test whether HSD2 neurons could similarly affect hedonic behaviors and anxiety, although our studies did not show a change in intake of sucrose consumption following HSD2 neuron activation[110]. These tests may be relevant for developing treatments for depression, as some studies in humans have found increased levels of aldosterone in depressed patients[163,164], and hyperaldosteronism is associated with increased anxiety[165,166] and depressive symptoms[167,168]. Determining what drives overconsumption of sodium could therefore have a large impact on public health.

References

1. Geerling, J. C. & Loewy, A. D. Central regulation of sodium appetite. *Exp. Physiol.* **93,** 177–209 (2008).

2. Orent-keiles, E., Robinson, A. & McCollum, E. V. The effects of sodium deprivation on the animal organism. *Am J Physiol.* 651–661 (1937).

3. Verbalis, J. G. Disorders of body water homeostasis. *Best Pract. Res. Clin. Endocrinol. Metab.* **17,** 471–503 (2003).

4. Fine, B. P., Ty, A., Lestrange, N. & Levine, O. R. Sodium deprivation growth failure in the rat: alterations in tissue composition and fluid spaces. *J. Nutr.* **117,** 1623–8 (1987).

5. Wolf, G. & Handal, P. J. Aldosterone-Induced Sodium Appetite: Dose-Response and Specificity. *Endocrinology* **78,** 1120–1124 (1966).

6. Nachman, M. Taste preferences for sodium salts by adrenalectomized rats. *J. Comp. Physiol. Psychol.* **55,** 1124–1129 (1962).

7. Richter, C. P. & Eckert, J. F. Mineral metabolism of adrenalectomized rats studied by the appetite method. *Endocrinology* **22,** 214–224 (1938).

8. Starr, L. J. & Rowland, N. E. Characteristics of salt appetite in chronically sodium-depleted rats using a progressive ratio schedule of procurement. *Physiol. Behav.* **88,** 433–442 (2006).

9. Wagman, W. Sodium chloride deprivation: development of sodium chloride as a reinforcement. *Science* **140,** 1403–4 (1963).

10. Quartermain, D., Miller, N. E. & Wolf, G. Role of experience in relationship between sodium deficiency and rate of bar pressing for salt. *J. Comp. Physiol. Psychol.* **63,** 417–20 (1967).

11. Berridge, K. C., Flynn, F. W., Schulkin, J. & Grill, H. J. Sodium depletion enhances salt palatability in rats. *Behav. Neurosci.* **98,** 652–60 (1984).

12. Alves, G., Sallé, J., Chaudy, S., Dupas, S. & Manière, G. High-NaCl perception in Drosophila melanogaster. *J. Neurosci.* **34,** 10884–91 (2014).

13. Liu, L. *et al.* Contribution of Drosophila DEG/ENaC Genes to Salt Taste. *Neuron* **39,** 133–146 (2003).

14. Oka, Y., Butnaru, M., von Buchholtz, L., Ryba, N. J. P. & Zuker, C. S. High salt recruits aversive taste pathways. *Nature* **494,** 472–5 (2013).

15. Zhang, Y. V, Ni, J. & Montell, C. The molecular basis for attractive salt-taste coding in Drosophila. *Science* **340,** 1334–8 (2013).

16. Chandrashekar, J. *et al.* The cells and peripheral representation of sodium taste in mice. *Nature* **464,** 297–301 (2010).

17. Bernstein, I. L. & Hennessy, C. J. Amiloride-sensitive sodium channels and expression of sodium appetite in rats. *Am. J. Physiol.* **253,** R371-4 (1987).

18. Breslin, P. A., Kaplan, J. M., Spector, A. C., Zambito, C. M. & Grill, H. J. Lick rate analysis of sodium taste-state combinations. *Am. J. Physiol.* **264,** R312-8 (1993).

19. St John, S. J. The Perceptual Characteristics of Sodium Chloride to Sodium-Depleted Rats. *Chem. Senses* **42,** 93–103 (2017).

20. Fortin, S. M. & Roitman, M. F. Challenges to body fluid homeostasis differentially recruit phasic dopamine signaling in a taste-selective manner. *J. Neurosci.* **38,** 6841–6853 (2018).

21. Cone, J. J. *et al.* Physiological state gates acquisition and expression of mesolimbic reward prediction signals. *Proc. Natl. Acad. Sci. U. S. A.* **113,** 1943–8 (2016).

22. Loriaux, A. L., Roitman, J. D. & Roitman, M. F. Nucleus accumbens shell, but not core, tracks motivational value of salt. *J. Neurophysiol.* **106,** 1537–1544 (2011).

23. Tindell, A. J., Smith, K. S., Peciña, S., Berridge, K. C. & Aldridge, J. W. Ventral Pallidum Firing Codes Hedonic Reward: When a Bad Taste Turns Good. *J. Neurophysiol.* **96,** 2399–2409 (2006).

24. Castro, D. C., Cole, S. L. & Berridge, K. C. Lateral hypothalamus, nucleus accumbens, and ventral pallidum roles in eating and hunger: interactions between homeostatic and reward circuitry. *Front. Syst. Neurosci.* **9,** 90 (2015).

25. Shimura, T., Imaoka, H. & Yamamoto, T. Neurochemical modulation of ingestive behavior in the ventral pallidum. *Eur. J. Neurosci.* **23,** 1596–604 (2006).

26. Cromwell, H. C. & Berridge, K. C. Where does damage lead to enhanced food aversion: the ventral pallidum/substantia innominata or lateral hypothalamus? *Brain Res.* **624,** 1–10 (1993).

27. Ho, C.-Y. & Berridge, K. C. Excessive disgust caused by brain lesions or temporary inactivations: mapping hotspots of the nucleus accumbens and ventral pallidum. *Eur. J. Neurosci.* **40,** 3556–72 (2014).

28. Chang, S. E., Smedley, E. B., Stansfield, K. J., Stott, J. J. & Smith, K. S. Optogenetic Inhibition of Ventral Pallidum Neurons Impairs Context-Driven Salt Seeking. *J. Neurosci.* **37,** 5670–5680 (2017).

29. Shibata, R., Kameishi, M., Kondoh, T. & Torii, K. Bilateral dopaminergic lesions in the ventral tegmental area of rats influence sucrose intake, but not umami and amino acid intake. *Physiol. Behav.* **96,** 667–674 (2009).

30. Wolf, G. Hypothalamic regulation of sodium intake: relations to preoptic and tegmental function. *Am. J. Physiol.* **213,** 1433–1438 (1967).

31. Liedtke, W. B. *et al.* Relation of addiction genes to hypothalamic gene changes subserving genesis and gratification of a classic instinct, sodium appetite. *Proc. Natl. Acad. Sci. U. S. A.* **108,** 12509–14 (2011).

32. Conover, K. L., Woodside, B. & Shizgal, P. Effects of sodium depletion on competition and summation between rewarding effects of salt and lateral hypothalamic stimulation in the rat. *Behav. Neurosci.* **108,** 549–558 (1994).

33. Bryant, R. W., Epstein, A. N., Fitzsimons, J. T. & Fluharty, S. J. Arousal of a specific and persistent sodium appetite in the rat with continuous intracerebroventricular infusion of angiotensin II. *J. Physiol.* **301,** 365–82 (1980).

34. Crews, E. C. & Rowland, N. E. Role of angiotensin in body fluid homeostasis of mice: effect of losartan on water and NaCl intakes. *Am. J. Physiol. Integr. Comp. Physiol.* **288,** R638–R644 (2005).

35. Sakai, R. R., Nicolaïdis, S. & Epstein, A. N. Salt appetite is suppressed by interference with angiotensin II and aldosterone. *Am. J. Physiol.* **251,** R762-8 (1986).

36. Matsuda, T. *et al.* Distinct neural mechanisms for the control of thirst and salt appetite in the

subfornical organ. *Nat. Neurosci.* **20,** 230–241 (2017).

37. Stricker, E. M., Gannon, K. S. & Smith, J. C. Salt appetite induced by DOCA treatment or adrenalectomy in rats: Analysis of ingestive behavior. *Physiol. Behav.* **52,** 793–802 (1992).

38. Richter, C. P. Increase salt appetite in adrenalectomized rats. *Am. J. Physiol.* **115,** 155–161 (1936).

39. Fluharty, S. J. & Epstein, A. N. Sodium appetite elicited by intracerebroventricular infusion of angiotensin II in the rat: II. Synergistic interaction with systemic mineralocorticoids. *Behav. Neurosci.* **97,** 746–758 (1983).

40. Formenti, S. *et al.* Hindbrain mineralocorticoid mechanisms on sodium appetite. *Am. J. Physiol. Regul. Integr. Comp. Physiol.* **304,** R252-9 (2013).

41. Rice, K. K. & Richter, C. P. Increased sodium chloride and water intake of normal rats treated with desoxycorticosterone acetate1. *Endocrinology* **33,** 106–115 (1943).

42. Geerling, J. C. & Loewy, A. D. Aldosterone-sensitive NTS neurons are inhibited by saline ingestion during chronic mineralocorticoid treatment. *Brain Res.* **1115,** 54–64 (2006).

43. Geerling, J. C., Kawata, M. & Loewy, A. D. Aldosterone-sensitive neurons in the rat central nervous system. *J. Comp. Neurol.* **494,** 515–27 (2006).

44. Reul, J. M. & de Kloet, E. R. Two receptor systems for corticosterone in rat brain: microdistribution and differential occupation. *Endocrinology* **117,** 2505–11 (1985).

45. Sheppard, K. E. & Funder, J. W. Equivalent affinity of aldosterone and corticosterone for type I receptors in kidney and hippocampus: direct binding studies. *J. Steroid Biochem.* **28,** 737–42 (1987).

46. Náray-Fejes-Tóth, A., Colombowala, I. K. & Fejes-Tóth, G. The role of 11beta-hydroxysteroid dehydrogenase in steroid hormone specificity. *J. Steroid Biochem. Mol. Biol.* **65,** 311–6 (1998).

47. Funder, J. W., Pearce, P. T., Smith, R. & Smith, A. I. Mineralocorticoid action: target tissue specificity is enzyme, not receptor, mediated. *Science* **242,** 583–5 (1988).

48. Chapman, K., Holmes, M. & Seckl, J. 11β-hydroxysteroid dehydrogenases: intracellular gate-keepers of tissue glucocorticoid action. *Physiol. Rev.* **93,** 1139–206 (2013).

49. Evans, L. C. *et al.* Conditional Deletion of Hsd11b2 in the Brain Causes Salt Appetite and Hypertension. *Circulation* **133,** 1360–70 (2016).

50. Ingram, M. C., Wallace, A. M., Collier, A., Fraser, R. & Connell, J. M. Sodium status, corticosteroid metabolism and blood pressure in normal human subjects and in a patient with abnormal salt appetite. *Clin. Exp. Pharmacol. Physiol.* **23,** 375–8 (1996).

51. Gasparini, S. *et al.* Aldosterone-sensitive HSD2 neurons in mice. *Brain Struct. Funct.* 1–31 (2018). doi:10.1007/s00429-018-1778-y

52. Roland, B. L., Li, K. X. & Funder, J. W. Hybridization histochemical localization of 11 beta-hydroxysteroid dehydrogenase type 2 in rat brain. *Endocrinology* **136,** 4697–4700 (1995).

53. Robson, A. C., Leckie, C. M., Seckl, J. R. & Holmes, M. C. 11β-Hydroxysteroid dehydrogenase type 2 in the postnatal and adult rat brain. *Mol. Brain Res.* **61,** 1–10 (1998).

54. Holmes, M. C. *et al.* 11β-Hydroxysteroid dehydrogenase type 2 protects the neonatal cerebellum from deleterious effects of glucocorticoids. *Neuroscience* **137,** 865–873 (2006).

55. Geerling, J. C. & Loewy, A. D. Sodium depletion activates the aldosterone-sensitive neurons in the NTS independently of thirst. *Am. J. Physiol. Regul. Integr. Comp. Physiol.* **292,** R1338-48 (2007).

56. Geerling, J. C. & Loewy, A. D. Sodium deprivation and salt intake activate separate neuronal subpopulations in the nucleus of the solitary tract and the parabrachial complex. *J. Comp. Neurol.* **504,** 379–403 (2007).

57. Broadwell, R. D. & Sofroniew, M. V. Serum Proteins Bypass the Blood-Brain Fluid Barriers for Extracellular Entry to the Central Nervous System. *Exp. Neurol.* **120,** 245–263 (1993).

58. Gross, P. M., Wall, K. M., Pang, J. J., Shaver, S. W. & Wainman, D. S. Microvascular specializations promoting rapid interstitial solute dispersion in nucleus tractus solitarius. *Am. J. Physiol.* **259,** R1131-8 (1990).

59. Resch, J. M. *et al.* Aldosterone-Sensing Neurons in the NTS Exhibit State-Dependent Pacemaker Activity and Drive Sodium Appetite via Synergy with Angiotensin II Signaling. *Neuron* **96,** 190–206.e7 (2017).

60. Wolf, G. Sodium appetite elicited by aldosterone. *Psychon. Sci.* **1,** 211–212 (1964).

61. Gasparini, S. *et al.* Rapid stimulation of sodium intake combining aldosterone into the 4th ventricle and the blockade of the lateral parabrachial nucleus. *Neuroscience* **346,** 94–101 (2017).

62. Shin, J.-W. & Loewy, A. D. Gastric afferents project to the aldosterone-sensitive HSD2 neurons of the NTS. *Brain Res.* **1301,** 34–43 (2009).

63. Shin, J.-W., Geerling, J. C. & Loewy, A. D. Vagal innervation of the aldosterone-sensitive HSD2 neurons in the NTS. *Brain Res.* **1249,** 135–47 (2009).

64. Nachman, M. & Valentino, D. A. Roles of taste and post-ingestional factors in the satiation of sodium appetite in rats. *J. Comp. Physiol. Psychol.* **62,** 280–283 (1966).

65. Sequeira, S. M., Geerling, J. C. & Loewy, A. D. Local inputs to aldosterone-sensitive neurons of the nucleus tractus solitarius. *Neuroscience* **141,** 1995–2005 (2006).

66. Curtis, K. S., Huang, W., Sved, A. F., Verbalis, J. G. & Stricker, E. M. Impaired osmoregulatory responses in rats with area postrema lesions. *Am. J. Physiol.* **277,** R209-19 (1999).

67. Kosten, T., Contreras, R. J., Stetson, P. W. & Ernest, M. J. Enhanced saline intake and decreased heart rate after area postrema ablations in rat. *Physiol. Behav.* **31,** 777–785 (1983).

68. Leshem, M. Biobehavior of the human love of salt. *Neurosci. Biobehav. Rev.* **33,** 1–17 (2009).

69. Beauchamp, G. K., Bertino, M., Burke, D. & Engelman, K. Experimental sodium depletion and salt taste in normal human volunteers. *Am. J. Clin. Nutr.* **51,** 881–9 (1990).

70. Kochli, A., Tenenbaum-Rakover, Y. & Leshem, M. Increased salt appetite in patients with congenital adrenal hyperplasia 21-hydroxylase deficiency. *Am. J. Physiol. Integr. Comp. Physiol.* **288,** R1673–R1681 (2005).

71. Leshem, M. Salt Preference in Adolescence Is Predicted by Common Prenatal and Infantile Mineralofluid Loss. *Physiol. Behav.* **63,** 699–704 (1998).

72. Leshem, M., Abutbul, A. & Eilon, R. Exercise Increases the Preference for Salt in Humans. *Appetite* **32,** 251–260 (1999).

73. Takamata, A., Mack, G. W., Gillen, C. M. & Nadel, E. R. Sodium appetite, thirst, and body fluid regulation in humans during rehydration without sodium replacement. *Am. J. Physiol.* **266,** R1493-502 (1994).

74. Leshem, M. & Rudoy, J. Hemodialysis increases the preference for salt in soup. *Physiol. Behav.* **61,** 65–69 (1997).

75. Jayedi, A., Ghomashi, F., Zargar, M. S. & Shab-Bidar, S. Dietary sodium, sodium-to-potassium ratio, and risk of stroke: A systematic review and nonlinear dose-response meta-analysis. *Clin. Nutr.* (2018). doi:10.1016/j.clnu.2018.05.017

76. Mozaffarian, D. *et al.* Global Sodium Consumption and Death from Cardiovascular Causes. *N. Engl. J. Med.* **371,** 624–634 (2014).

77. Strazzullo, P., D'Elia, L., Kandala, N.-B. & Cappuccio, F. P. Salt intake, stroke, and cardiovascular disease: meta-analysis of prospective studies. *BMJ* **339,** b4567 (2009).

78. Philipson, H., Ekman, I., Forslund, H. B., Swedberg, K. & Schaufelberger, M. Salt and fluid restriction is effective in patients with chronic heart failure. *Eur. J. Heart Fail.* **15,** 1304–1310 (2013).

79. Alvelos, M. *et al.* The effect of dietary sodium restriction on neurohumoral activity and renal dopaminergic response in patients with heart failure. *Eur. J. Heart Fail.* **6,** 593–599 (2004).

80. Garofalo, C. *et al.* Dietary Salt Restriction in Chronic Kidney Disease: A Meta-Analysis of Randomized Clinical Trials. *Nutrients* **10,** 732 (2018).

81. Korhonen, M. H. *et al.* Adherence to the salt restriction diet among people with mildly elevated blood pressure. *Eur. J. Clin. Nutr.* **53,** 880–5 (1999).

82. Ohta, Y. *et al.* Relationship between the awareness of salt restriction and the actual salt intake in hypertensive patients. *Hypertens. Res.* **27,** 243–6 (2004).

83. Takahashi, N. *et al.* Awareness of salt restriction is not reflected in the actual salt intake in Japanese hypertensive patients. *Clin. Exp. Hypertens.* **37,** 388–392 (2015).

84. Luquet, S., Perez, F. a, Hnasko, T. S. & Palmiter, R. D. NPY/AgRP neurons are essential for feeding in adult mice but can be ablated in neonates. *Science* **310,** 683–5 (2005).

85. Oka, Y., Ye, M. & Zuker, C. S. Thirst driving and suppressing signals encoded by distinct neural populations in the brain. *Nature* **520,** 349–52 (2015).

86. Aponte, Y., Atasoy, D. & Sternson, S. M. AGRP neurons are sufficient to orchestrate feeding behavior rapidly and without training. *Nat. Neurosci.* **14,** 351–5 (2011).

87. Rogan, S. C. & Roth, B. L. Remote control of neuronal signaling. *Pharmacol. Rev.* **63,** 291–315 (2011).

88. Sakai, R. R., Frankmann, S. P., Fine, W. B. & Epstein, A. N. Prior episodes of sodium depletion increase the need-free sodium intake of the rat. *Behav. Neurosci.* **103,** 186–92 (1989).

89. Antunes-Rodrigues, J., De Castro, M., Elias, L. L. K., Valença, M. M. & McCann, S. M. Neuroendocrine Control of Body Fluid Metabolism. *Physiol. Rev.* **84,** (2004).

90. Dadam, F. M. *et al.* Effect of sex chromosome complement on sodium appetite and Fos-immunoreactivity induced by sodium depletion. *Am. J. Physiol. Regul. Integr. Comp. Physiol.* **306,** R175-84 (2014).

91. Kim, J. C. *et al.* Linking Genetically Defined Neurons to Behavior through a Broadly Applicable Silencing Allele. *Neuron* **63,** 305–315 (2009).

92. Breslin, P. A., Spector, A. C. & Grill, H. J. Chorda tympani section decreases the cation specificity of depletion-induced sodium appetite in rats. *Am. J. Physiol.* **264,** R319-23 (1993).

93. Krashes, M. J. *et al.* Rapid, reversible activation of AgRP neurons drives feeding behavior in mice. *J. Clin. Invest.* **121,** 1424–8 (2011).

94. Geerling, J. C. & Loewy, A. D. Aldosterone-sensitive neurons in the nucleus of the solitary: efferent projections. *J. Comp. Neurol.* **498,** 223–50 (2006).

95. Geerling, J. C. *et al.* FoxP2 expression defines dorsolateral pontine neurons activated by sodium deprivation. *Brain Res.* **1375,** 19–27 (2011).

96. Menani, J. V, De Luca, L. A. & Johnson, A. K. Role of the lateral parabrachial nucleus in the control of sodium appetite. *Am. J. Physiol. Regul. Integr. Comp. Physiol.* **306,** R201-10 (2014).

97. Betley, J. N., Cao, Z. F. H., Ritola, K. D. & Sternson, S. M. Parallel, Redundant Circuit Organization for Homeostatic Control of Feeding Behavior. *Cell* **155,** 1337–1350 (2013).

98. Nation, H. L. *et al.* DREADD-induced activation of subfornical organ neurons stimulates thirst and salt appetite. *J. Neurophysiol.* **115,** 3123–9 (2016).

99. Gore, B. B., Soden, M. E. & Zweifel, L. S. Manipulating gene expression in projection-specific neuronal populations using combinatorial viral approaches. *Curr. Protoc. Neurosci.* **4,** 4.35.1-4.35.20 (2013).

100. Geerling, J. C. *et al.* Genetic identity of thermosensory relay neurons in the lateral parabrachial nucleus. *Am. J. Physiol. Regul. Integr. Comp. Physiol.* **310,** R41-54 (2016).

101. Juan De Solis, A., Baquero, A. F., Bennett, C. M., Grove, K. L. & Zeltser, L. M. Postnatal undernutrition delays a key step in the maturation of hypothalamic feeding circuits. *Mol. Metab.* **5,** 198–209 (2016).

102. Ma, C.-W. *et al.* Postnatal expression of TrkB receptor in rat vestibular nuclear neurons responsive to horizontal and vertical linear accelerations. *J. Comp. Neurol.* **521,** 612–625 (2013).

103. Enjin, A. *et al.* Identification of novel spinal cholinergic genetic subtypes disclose Chodl and Pitx2 as markers for fast motor neurons and partition cells. *J. Comp. Neurol.* **518,** 2284–2304 (2010).

104. Bochorishvili, G., Stornetta, R. L., Coates, M. B. & Guyenet, P. G. Pre-Bötzinger complex receives glutamatergic innervation from galaninergic and other retrotrapezoid nucleus neurons. *J. Comp. Neurol.* **520,** 1047–1061 (2012).

105. Rowland, N. E., Farnbauch, L. J. & Crews, E. C. Sodium deficiency and salt appetite in ICR: CD1 mice. *Physiol. Behav.* **80,** 629–35 (2004).

106. Flynn, F. W., Grill, H. J., Schulkin, J. & Norgren, R. Central gustatory lesions: II. Effects on sodium appetite, taste aversion learning, and feeding behaviors. *Behav. Neurosci.* **105,** 944–954 (1991).

107. Scalera, G., Spector, A. C. & Norgren, R. Excitotoxic lesions of the parabrachial nuclei prevent conditioned taste aversions and sodium appetite in rats. *Behav. Neurosci.* **109,** 997–1008 (1995).

108. Stricker, E. M., Grigson, P. S. & Norgren, R. Variable effects of parabrachial nucleus lesions on salt appetite in rats depending upon experimental paradigm and saline concentration. *Behav.*

Neurosci. **127,** 275–284 (2013).

109. Nishijo, H. & Norgren, R. Responses from parabrachial gustatory neurons in behaving rats. *J Neurophysiol* **63,** 707–724 (1990).

110. Jarvie, B. C. & Palmiter, R. D. HSD2 neurons in the hindbrain drive sodium appetite. *Nat. Neurosci.* **20,** 167–169 (2017).

111. Rousso, D. L. *et al.* Two Pairs of ON and OFF Retinal Ganglion Cells Are Defined by Intersectional Patterns of Transcription Factor Expression. *Cell Rep.* **15,** 1930–1944 (2016).

112. Shin, J.-W., Geerling, J. C., Stein, M. K., Miller, R. L. & Loewy, A. D. FoxP2 brainstem neurons project to sodium appetite regulatory sites. *J. Chem. Neuroanat.* **42,** 1–23 (2011).

113. Miller, R. L. *et al.* Fos-activation of FoxP2 and Lmx1b neurons in the parabrachial nucleus evoked by hypotension and hypertension in conscious rats. *Neuroscience* **218,** 110–125 (2012).

114. Ryan, P. J., Ross, S. I., Campos, C. A., Derkach, V. A. & Palmiter, R. D. Oxytocin-receptor-expressing neurons in the parabrachial nucleus regulate fluid intake. *Nat. Neurosci.* **20,** 1722–1733 (2017).

115. Gray, P. A. Transcription factors and the genetic organization of brain stem respiratory neurons. *J. Appl. Physiol.* **104,** 1513–1521 (2008).

116. Andrade, C. A. F., Barbosa, S. P., De Luca, L. A. & Menani, J. V. Activation of α2-adrenergic receptors into the lateral parabrachial nucleus enhances NaCl intake in rats. *Neuroscience* **129,** 25–34 (2004).

117. Pavan, C. G. *et al.* Activation of μ opioid receptors in the LPBN facilitates sodium intake in rats. *Behav. Brain Res.* **288,** 20–25 (2015).

118. Menani, J. V, Thunhorst, R. L. & Johnson, A. K. Lateral parabrachial nucleus and serotonergic mechanisms in the control of salt appetite in rats. *Am. J. Physiol.* **270,** R162-8 (1996).

119. De Oliveira, L. B., De Luca, L. A. & Menani, J. V. Opioid activation in the lateral parabrachial nucleus induces hypertonic sodium intake. *Neuroscience* **155,** 350–358 (2008).

120. Callera, J. C. *et al.* GABA(A) receptor activation in the lateral parabrachial nucleus induces water and hypertonic NaCl intake. *Neuroscience* **134,** 725–35 (2005).

121. Callera, J. C. *et al.* GABAA receptor activation in the lateral parabrachial nucleus induces water and hypertonic NaCl intake. *Neuroscience* **134,** 725–735 (2005).

122. Andrade-Franzé, G. M. F. *et al.* Lesions in the central amygdala impair sodium intake induced by the blockade of the lateral parabrachial nucleus. *Brain Res.* **1332,** 57–64 (2010).

123. Menani, J. V., Barbosa, S. P., De Luca, L. A., De Gobbi, J. I. F. & Johnson, A. K. Serotonergic mechanisms of the lateral parabrachial nucleus and cholinergic-induced sodium appetite. *Am. J. Physiol. Integr. Comp. Physiol.* **282,** R837–R841 (2002).

124. Menani, J. V, De Luca, L. A. & Johnson, A. K. Lateral parabrachial nucleus serotonergic mechanisms and salt appetite induced by sodium depletion. *Am. J. Physiol.* **274,** R555-60 (1998).

125. Colombari, D. S., Menani, J. V & Johnson, A. K. Forebrain angiotensin type 1 receptors and parabrachial serotonin in the control of NaCl and water intake. *Am. J. Physiol.* **271,** R1470-6 (1996).

126. Reilly, J. J., Maki, R., Nardozzi, J. & Schulkin, J. The effects of lesions of the bed nucleus of the stria terminalis on sodium appetite. *Acta Neurobiol. Exp. (Wars).* **54,** 253–7 (1994).

127. Johnson, A. K., de Olmos, J., Pastuskovas, C. V, Zardetto-Smith, A. M. & Vivas, L. The extended amygdala and salt appetite. *Ann. N. Y. Acad. Sci.* **877,** 258–80 (1999).

128. Zardetto-Smith, A. M., Beltz, T. G. & Johnson, A. K. Role of the central nucleus of the amygdala and bed nucleus of the stria terminalis in experimentally-induced salt appetite. *Brain Res.* **645,** 123–134 (1994).

129. Epstein, A. N. The dependence of the salt appetite of the rat on the hormonal consequences of sodium deficiency. *J. Physiol. (Paris).* **79,** 496–8 (1984).

130. Geerling, J. C. & Loewy, A. D. Sodium depletion activates the aldosterone-sensitive neurons in the NTS independently of thirst. *Am. J. Physiol. Integr. Comp. Physiol.* **292,** R1338–R1348 (2007).

131. Geerling, J. C., Engeland, W. C., Kawata, M. & Loewy, A. D. Aldosterone target neurons in the nucleus tractus solitarius drive sodium appetite. *J. Neurosci.* **26,** 411–7 (2006).

132. Sakai, R. R. & Epstein, A. N. Dependence of adrenalectomy-induced sodium appetite on the action of angiotensin II in the brain of the rat. *Behav. Neurosci.* **104,** 167–176 (1990).

133. Galaverna, O. *et al.* Blockade of central angiotensin II type 1 and type 2 receptors suppresses adrenalectomy-induced NaCl intake in rats. *Regul. Pept.* **66,** 47–50 (1996).

134. Weisinger, R. S. *et al.* Subfornical organ lesion decreases sodium appetite in the sodium-depleted rat. *Brain Res.* **526,** 23–30 (1990).

135. Wilson, W. L., Starbuck, E. M. & Fitts, D. A. Salt appetite of adrenalectomized rats after a lesion of the SFO. *Behav. Brain Res.* **136,** 449–453 (2002).

136. Nation, H. L., Nicoleau, M., Kinsman, B. J., Browning, K. N. & Stocker, S. D. DREADD-induced activation of subfornical organ neurons stimulates thirst and salt appetite. *J. Neurophysiol.* **115,** 3123–3129 (2016).

137. Leib, D. E. *et al.* The Forebrain Thirst Circuit Drives Drinking through Negative Reinforcement. *Neuron* **96,** 1272–1281.e4 (2017).

138. Shimizu, H. *et al.* Glial Nax Channels Control Lactate Signaling to Neurons for Brain [Na+] Sensing. *Neuron* **54,** 59–72 (2007).

139. Watanabe, E. *et al.* Nav2/NaG channel is involved in control of salt-intake behavior in the CNS. *J. Neurosci.* **20,** 7743–51 (2000).

140. Hiyama, T. Y., Watanabe, E., Okado, H. & Noda, M. The subfornical organ is the primary locus of sodium-level sensing by Na(x) sodium channels for the control of salt-intake behavior. *J. Neurosci.* **24,** 9276–81 (2004).

141. Fitts, D. A. Effects of lesions of the ventral ventral median preoptic nucleus or subfornical organ on drinking and salt appetite after deoxycorticosterone acetate or yohimbine. *Behav. Neurosci.* **105,** 721–6 (1991).

142. Chen, J. Y., Campos, C. A., Jarvie, B. C. & Palmiter, R. D. Parabrachial CGRP Neurons Establish and Sustain Aversive Taste Memories. *Neuron* **100,** (2018).

143. Dietrich, M. O., Zimmer, M. R., Bober, J. & Horvath, T. L. Hypothalamic Agrp Neurons Drive

Stereotypic Behaviors beyond Feeding. *Cell* **160,** 1222–1232 (2015).

144. Padilla, S. L. *et al.* Agouti-related peptide neural circuits mediate adaptive behaviors in the starved state. *Nat. Neurosci.* **19,** 734–741 (2016).

145. Alhadeff, A. L. *et al.* A Neural Circuit for the Suppression of Pain by a Competing Need State. *Cell* **173,** 140–152.e15 (2018).

146. Galaverna, O. G. *et al.* Lesions of the central nucleus of the amygdala. I: Effects on taste reactivity, taste aversion learning and sodium appetite. *Behav. Brain Res.* **59,** 11–7 (1993).

147. Tandon, S., Simon, S. A. & Nicolelis, M. A. L. Appetitive changes during salt deprivation are paralleled by widespread neuronal adaptations in nucleus accumbens, lateral hypothalamus, and central amygdala. *J. Neurophysiol.* **108,** 1089–1105 (2012).

148. Roitman, M. F., Na, E., Anderson, G., Jones, T. A. & Bernstein, I. L. Induction of a salt appetite alters dendritic morphology in nucleus accumbens and sensitizes rats to amphetamine. *J. Neurosci.* **22,** RC225 (2002).

149. Dalmasso, C., Antunes-Rodrigues, J., Vivas, L. & De Luca, L. A. Mapping brain Fos immunoreactivity in response to water deprivation and partial rehydration: Influence of sodium intake. *Physiol. Behav.* **151,** 494–501 (2015).

150. Lucas, L. R., Grillo, C. A. & McEwen, B. S. Involvement of mesolimbic structures in short-term sodium depletion: in situ hybridization and ligand-binding analyses. *Neuroendocrinology* **77,** 406–15 (2003).

151. Wirtshafter, D., Covelo, I. R., Salija, I. & Stratford, T. R. Effects of muscimol in the nucleus accumbens shell on salt appetite and sucrose intake: A microstructural study with a comment on the sensitization of salt intake. *Behav. Neurosci.* **126,** 699–709 (2012).

152. Gomez-Sanchez, E. P. Intracerebroventricular infusion of aldosterone induces hypertension in rats. *Endocrinology* **118,** 819–823 (1986).

153. Gómez-Sánchez, E. P., Fort, C. M. & Gómez-Sánchez, C. E. Intracerebroventricular infusion of RU28318 blocks aldosterone-salt hypertension. *Am. J. Physiol.* **258,** E482-4 (1990).

154. Gasparini, S. *et al.* Aldosterone infusion into the 4th ventricle produces sodium appetite with baroreflex attenuation independent of renal or blood pressure changes. *Brain Res.* **1698,** 70–80 (2018).

155. Bolhuis, D. P., Costanzo, A., Newman, L. P. & Keast, R. S. Salt Promotes Passive Overconsumption of Dietary Fat in Humans. *J. Nutr.* **146,** 838–845 (2015).

156. Deglaire, A. *et al.* Associations between weight status and liking scores for sweet, salt and fat according to the gender in adults (The Nutrinet-Santé study). *Eur. J. Clin. Nutr.* **69,** 40–46 (2015).

157. Yoon, Y. S. & Oh, S. W. Sodium density and obesity; the Korea National Health and Nutrition Examination Survey 2007–2010. *Eur. J. Clin. Nutr.* **67,** 141–146 (2013).

158. Grippo, A. J., Moffitt, J. A., Beltz, T. G. & Johnson, A. K. Reduced hedonic behavior and altered cardiovascular function induced by mild sodium depletion in rats. *Behav. Neurosci.* **120,** 1133–1143 (2006).

159. Morris, M. J., Na, E. S. & Johnson, A. K. Mineralocorticoid receptor antagonism prevents hedonic deficits induced by a chronic sodium appetite. *Behav. Neurosci.* **124,** 211–224 (2010).

160. Morris, M. J., Na, E. S., Grippo, A. J. & Johnson, A. K. The effects of deoxycorticosterone-induced sodium appetite on hedonic behaviors in the rat. *Behav. Neurosci.* **120,** 571–579 (2006).

161. Hlavacova, N. *et al.* Subchronic treatment with aldosterone induces depression-like behaviours and gene expression changes relevant to major depressive disorder. *Int. J. Neuropsychopharmacol.* **15,** 247–265 (2012).

162. Hlavacova, N. & Jezova, D. Chronic treatment with the mineralocorticoid hormone aldosterone results in increased anxiety-like behavior. *Horm. Behav.* **54,** 90–97 (2008).

163. Murck, H. *et al.* The Renin-Angiotensin-Aldosterone system in patients with depression compared to controls – a sleep endocrine study. *BMC Psychiatry* **3,** 15 (2003).

164. Emanuele, E., Geroldi, D., Minoretti, P., Coen, E. & Politi, P. Increased Plasma Aldosterone in Patients with Clinical Depression. *Arch. Med. Res.* **36,** 544–548 (2005).

165. Sonino, N. *et al.* Psychological Assessment of Primary Aldosteronism: A Controlled Study. *J. Clin. Endocrinol. Metab.* **96,** E878–E883 (2011).

166. Sonino, N., Fallo, F. & Fava, G. A. Psychological aspects of primary aldosteronism. *Psychother. Psychosom.* **75,** 327–30 (2006).

167. Reincke, M. Anxiety, Depression, and Impaired Quality of Life in Primary Aldosteronism: Why We Shouldn't Ignore It! *J. Clin. Endocrinol. Metab.* **103,** 1–4 (2018).

168. Velema, M. *et al.* Health-Related Quality of Life and Mental Health in Primary Aldosteronism: A Systematic Review. *Horm. Metab. Res.* **49,** 943–950 (2017).

169. Padilla, S. L., Johnson, C. W., Barker, F. D., Patterson, M. A. & Palmiter, R. D. A Neural Circuit Underlying the Generation of Hot Flushes. *Cell Rep.* **24,** 271–277 (2018).

Appendix I: Foxp2 neurons in the PBN and pre-LC are involved in thermoregulation.

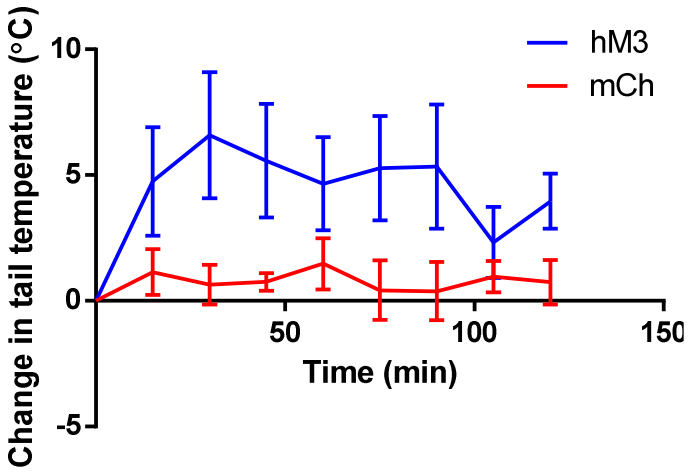

Activation of Foxp2 neurons in the PBN/pre-LC increases tail-skin temperature.

Foxp2$^{Cre/+}$ mice were transduced with a Cre-dependent virus driving expression of mCherry (mCh) or hM3Dq:mCherry (hM3) in the PBN and pre-LC (n = 4/group). These are the same mice used elsewhere in this document. Mice were given peripheral injections of CNO (1 mg/kg) at time 0, and measurements of tail skin temperature were taken every 15 min for 2 h, starting an hour after the start of the dark cycle. There was not a significant increase in tail skin temperature (Two-way RM ANOVA, interaction $F(8, 48) = 1.421$, $P = 0.2121$), although there is a clear trend for what is a 5°C change in tail-skin temperature.

Tail-skin temperature was recorded using an infrared camera (FLIR E4; FLIR Instruments) and analyzed with the software provide (FLIR Tools) and a custom Python script as previously described[169].

These data were collected in collaboration with Chris Johnson.

Reference:

169. Padilla, S. L., Johnson, C. W., Barker, F. D., Patterson, M. A. & Palmiter, R. D. A Neural Circuit Underlying the Generation of Hot Flushes. *Cell Rep.* **24,** 271–277 (2018).

Appendix II: Morphine, *Oprm1* and *Calca* in the PBN, and salt intake

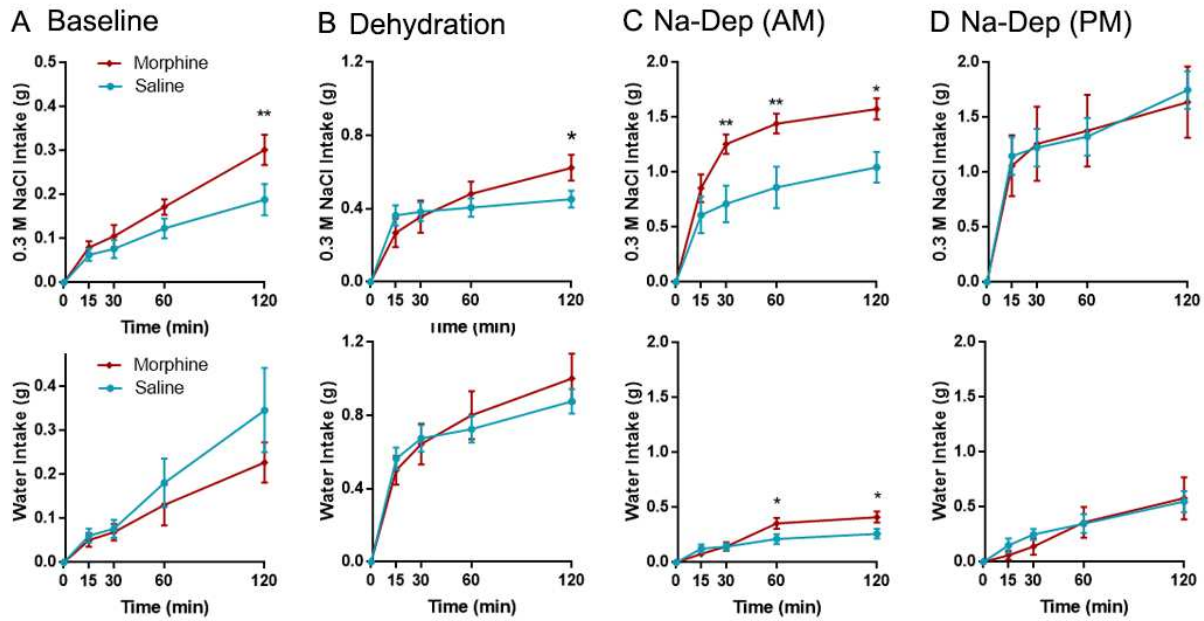

Peripheral morphine can increase sodium intake

Wild-type mice were given a peripheral injection of morphine (1.5 mg/kg, n = 9) or saline (n = 8) 30 min before presentation of 0.3 M NaCl and water in a two-bottle choice test under various conditions. (A) Morphine increased baseline intake of NaCl but not water during the first 2 h of the dark cycle compared to mice treated with saline injections (Two-way RM ANOVA, *post hoc* Sidak's multiple comparisons test; salt, interaction $F(4, 32) = 1.953$, $P = 0.1256$; water, interaction $F(4, 32) = 0.837$, $P = 0.5119$). (B) Morphine also increased intake of salt but not water following overnight dehydration (Two-way RM ANOVA, post-hoc Sidak's multiple comparisons test; salt, interaction $F(4, 28) = 2.959$, $P = 0.037$; water, interaction $F(4, 32) = 1.994$, $P = 0.1192$). (C-D) Mice were sodium depleted (Na-Dep) by treatment with two injections of furosemide spaced 24-h apart, followed by presentation of sodium and water either during the day (C) or during the dark cycle (D). Increases in intake of both water and salt occurred during the day (Two-way RM ANOVA, post-hoc Sidak's multiple comparisons test; salt, interaction $F(4, 60) = 5.964$, $P = 0.0004$. water; interaction $F(4, 60) = 6.128$, $P = 0.0003$), but not when the solutions were presented at the start of the dark cycle (Two-way RM ANOVA, interaction $F(4, 32) = 1.953$, $P = 0.1256$; water, interaction $F(4, 32) = 0.8370$, $P = 0.5119$). * $P < .05$, ** $P < .01$.

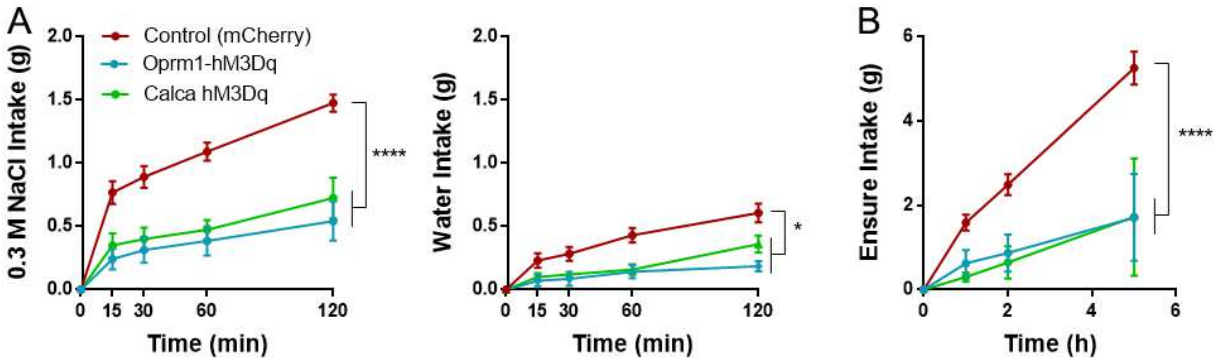

Activation of *Oprm1* and *Calca* neurons in the PBN inhibit sodium intake

The mu-opioid receptor is encoded by the gene *Oprm1*. *Oprm1*$^{Cre/+}$ or *Calca*$^{Cre/+}$ mice were transduced with either AAV1-DIO-mCherry (mCherry) or AAV1-DIO-hM3Dq:mCherry (hM3Dq) in the LPBN. (A)Mice were sodium depleted with with furosemide as described in Chapter 2, and then given peripheral injections of 1 mg/kg CNO 30 min prior to the start of the dark cycle, and mice underwent a two-bottle choice test with access to either 0.3 M NaCl or water. Activation of both *Oprm1*(n = 7) and *Calca* (n = 4) neurons in the PBN decreased intake of both salt and water compared to controls (n = 13). (Two-way RM ANOVA, *post hoc* Sidak's multiple comparisons test; salt, interaction $F(8, 84) = 9.986$, $P < 0.0001$; water, interaction $F(8, 88) = 5.135$, $P < 0.0001$). (B) Activation of both *Oprm1* and *Calca* neurons in the PBN decreased intake of ensure. (Two-way RM ANOVA, *post hoc* Sidak's multiple comparisons test; salt, interaction $F(6, 63) = 8.070$, $P < 0.0001$). * $P < 0.05$, ****$P < 0.0001$.